

Master Thesis

**Exploring the existence of prebiotic species:
ALMA observations of amine-containing
organic molecule in star-forming regions.**

Harumi Minamoto

17M01629

Nomura Laboratory

Department of Earth and Planetary Sciences, Tokyo Institute of Technology

January 11, 2019

Abstract

L A variety of complex organic molecules have been observed for decades in the interstellar medium. Some of them are considered to be delivered to the primordial Earth by comets, and contributed to the chemical evolution leading to terrestrial life. One example of such prebiotic species is amino acid. Glycine, the simplest amino acid, has been detected in comet 67P/C-G but its presence in molecular clouds is still uncertain.

In this work we analyze the ALMA archival data toward 3 star-forming regions, Orion Kleinmann-Low nebula (hereafter Orion-KL), IRAS 16293-2422 (IRAS 16293), and L483, to search methylamine (CH_3NH_2), which is suggested as precursors to glycine.

As a result of analysis, we found 8 candidate emission at the hot core region in Orion-KL. By using the rotation diagram method, we evaluated its tentative column density and rotational temperature to be $5.5 \times 10^{14} \text{ cm}^{-2}$ and 93.3 K, respectively. On the other hand, CH_3NH_2 is not detected and stringent upper limit column densities are determined in IRAS 16293 and L483.

Contents

Abstract	i
1 Introduction	1
1.1 Glycine and methylamine	1
1.2 Star forming region	1
1.2.1 Orion Kleinmann-Low nebula	1
1.2.2 IRAS 16293-2422	1
1.2.3 L483	1
1.3 Radio observation	1
1.3.1 Atacama Large Millimeter Array	1
1.4 Purpose of this work	1
2 Methylamine survey in Orion-KL	2
2.1 Observation data	2
2.2 Analysis	2
2.2.1 Continuum Subtraction of SV data	2
2.2.2 Line identification	2
2.3 Results	3
2.3.1 Transitions	3
2.3.2 Distribution	3
2.3.3 Spectrum	5
2.4 Disucssion	5

2.4.1	Column density and Rotation temperature	5
2.4.2	Blending	5
3	Methylamine survey in low mass star-forming regions	16
3.1	Review of low mass star-forming region	16
3.2	Analysis	16
3.3	IRAS 16293	16
3.3.1	Observation data	16
3.3.2	Results	16
3.4	L483	16
3.4.1	Observation data	16
3.4.2	Results	16
4	Discussion	18
5	Conclusions	19
A	Distribution of methylamine lines contaminated by other molecular line emission in Orion-KL	20
A.1	Integrated intensity maps	20
A.2	Channel maps	24
Acknowledgments		40
References		41

Chapter 1

Introduction

1.1 Glycine and methylamine

1.2 Star forming region

1.2.1 Orion Kleinmann-Low nebula

1.2.2 IRAS 16293-2422

1.2.3 L483

1.3 Radio observation

1.3.1 Atacama Large Millimeter Array

1.4 Purpose of this work

Chapter 2

Methylamine survey in Orion-KL

2.1 Observation data

2.2 Analysis

2.2.1 Continuum Subtraction of SV data

2.2.2 Line identification

1. We drew methylamine emission maps using Common Astronomy Software Applications (CASA) software (McMullin et al. 2007). We used JPL Molecular Spectroscopy catalog to identify the transition lines. 8 spectral features exhibit a compact emission at the center of the Hot core . We extracted spectrum from this region.

2. We estimated the systemic velocity and the line width of 217.758 GHz line, reported by Pagani et al. (2017), which seem contaminated by other lines.
3. Using these value, we obtained the integrated intensity of 8 transitions described in Table 2.1 by Gaussian fitting.

2.3 Results

2.3.1 Transitions

Table 2.1: Observed rotational transitions of CH₃NH₂ in Orion-KL

Frequency [GHz]	Sμ ² [D ²]	E _u [K]	Transition (J, K_a, Γ)	Comments
215.670	53.92	111.48	9, 2, $E_{1-1} \rightarrow 9, 1, E_{1+1}$	
245.202	37.84	168.31	12, 1, $B_2 \rightarrow 11, 2, B_1$	
217.758	129.88	182.05	12, 2, $B_2 \rightarrow 12, 1, B_1$	
221.755	35.06	133.11	10, 2, $A_2 \rightarrow 10, 1, A_1$	
229.908	27.37	92.71	8, 2, $A_2 \rightarrow 8, 1, A_1$	
235.735	82.06	92.76	8, 2, $B_2 \rightarrow 8, 1, B_1$	
242.262	60.23	60.86	6, 2, $B_2 \rightarrow 6, 1, B_1$	
244.887	49.54	48.09	5, 2, $B_1 \rightarrow 5, 1, B_2$	

2.3.2 Distribution

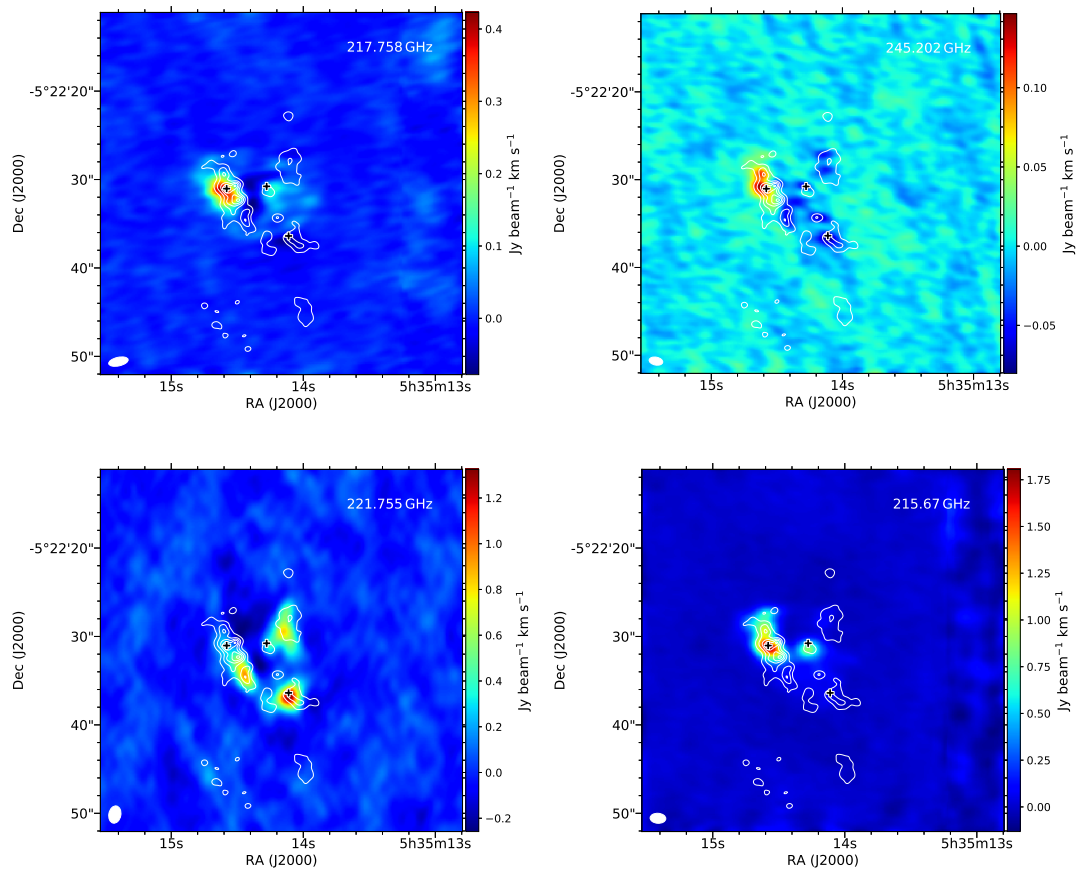


Figure 2.1: Integrated intensity map

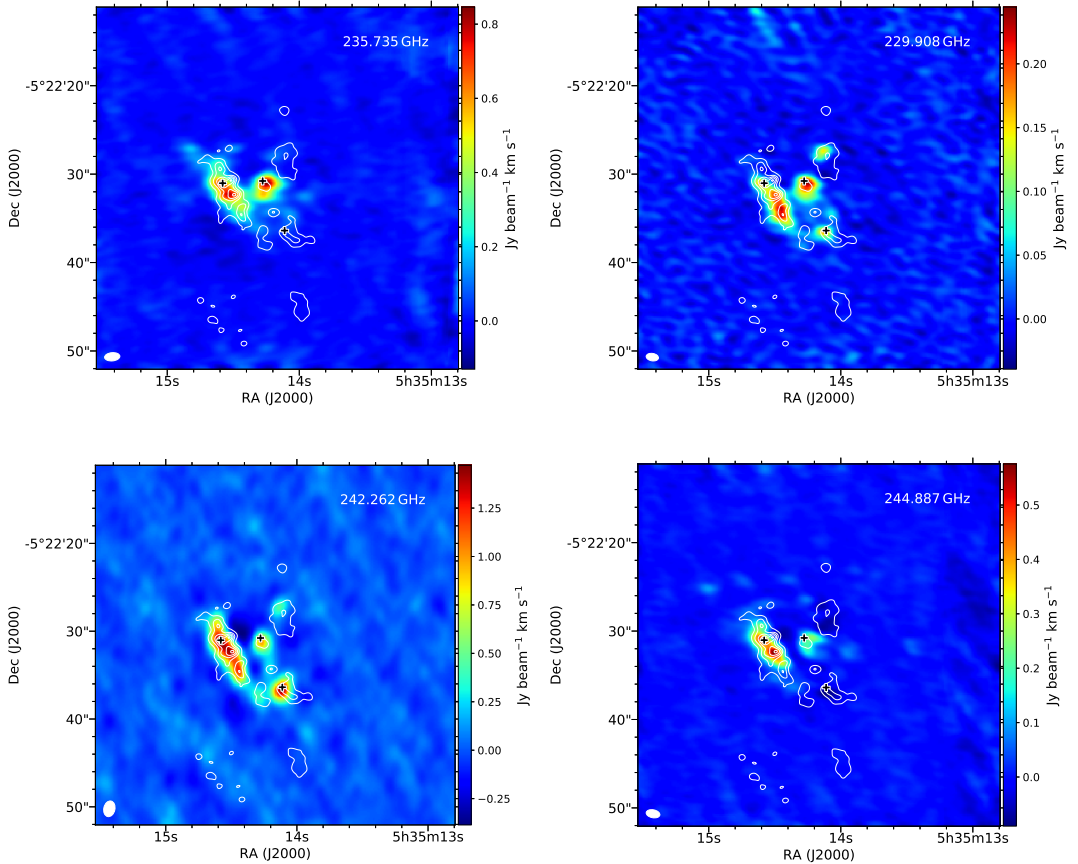


Figure 2.2: (Continued)

2.3.3 Spectrum

2.4 Disucssion

2.4.1 Column density and Rotation temperature

In this subsection we will describe the methodologies in deriving fractional abundances of COMs.

2.4.2 Blending

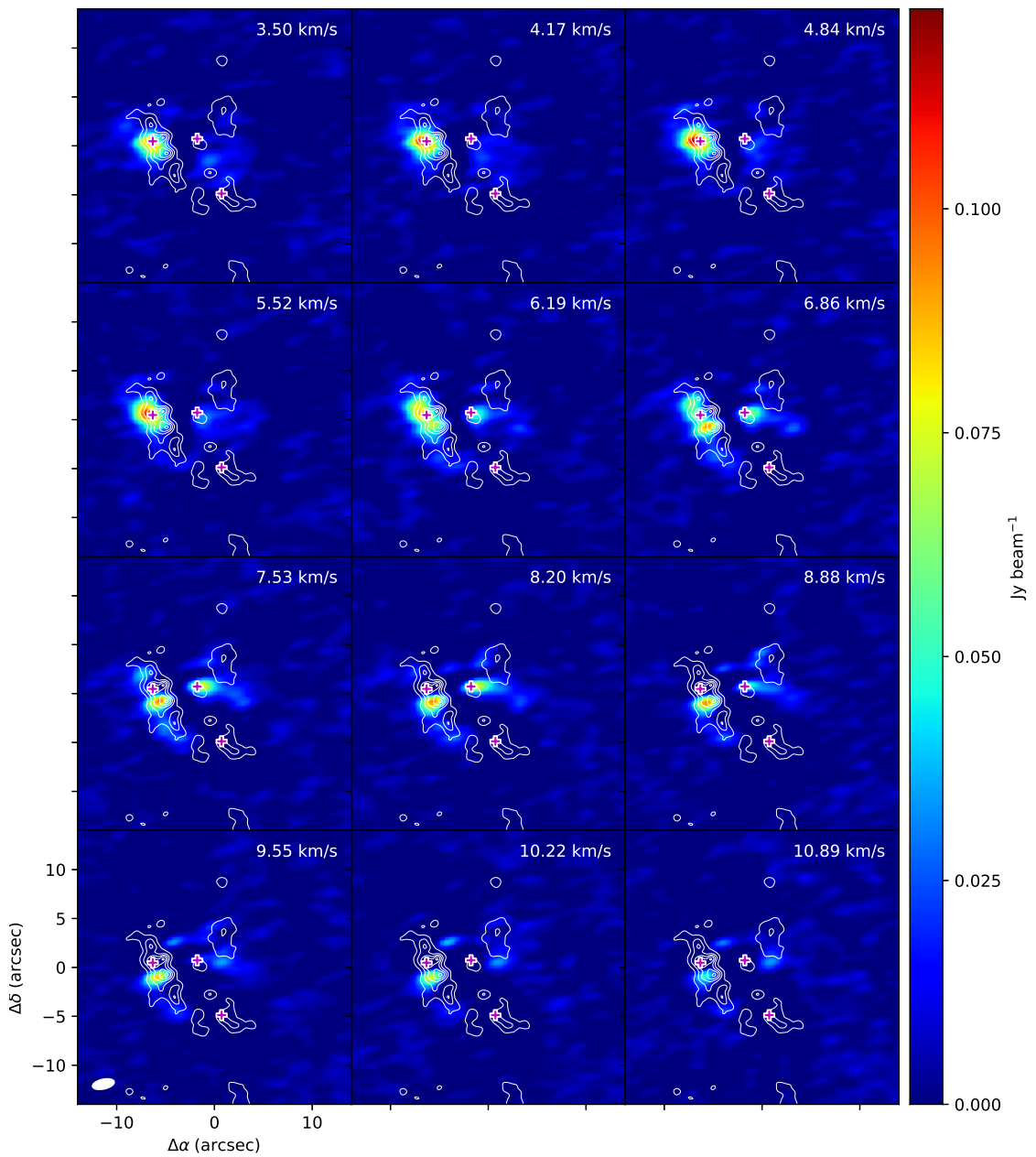


Figure 2.3: 217.758 GHz

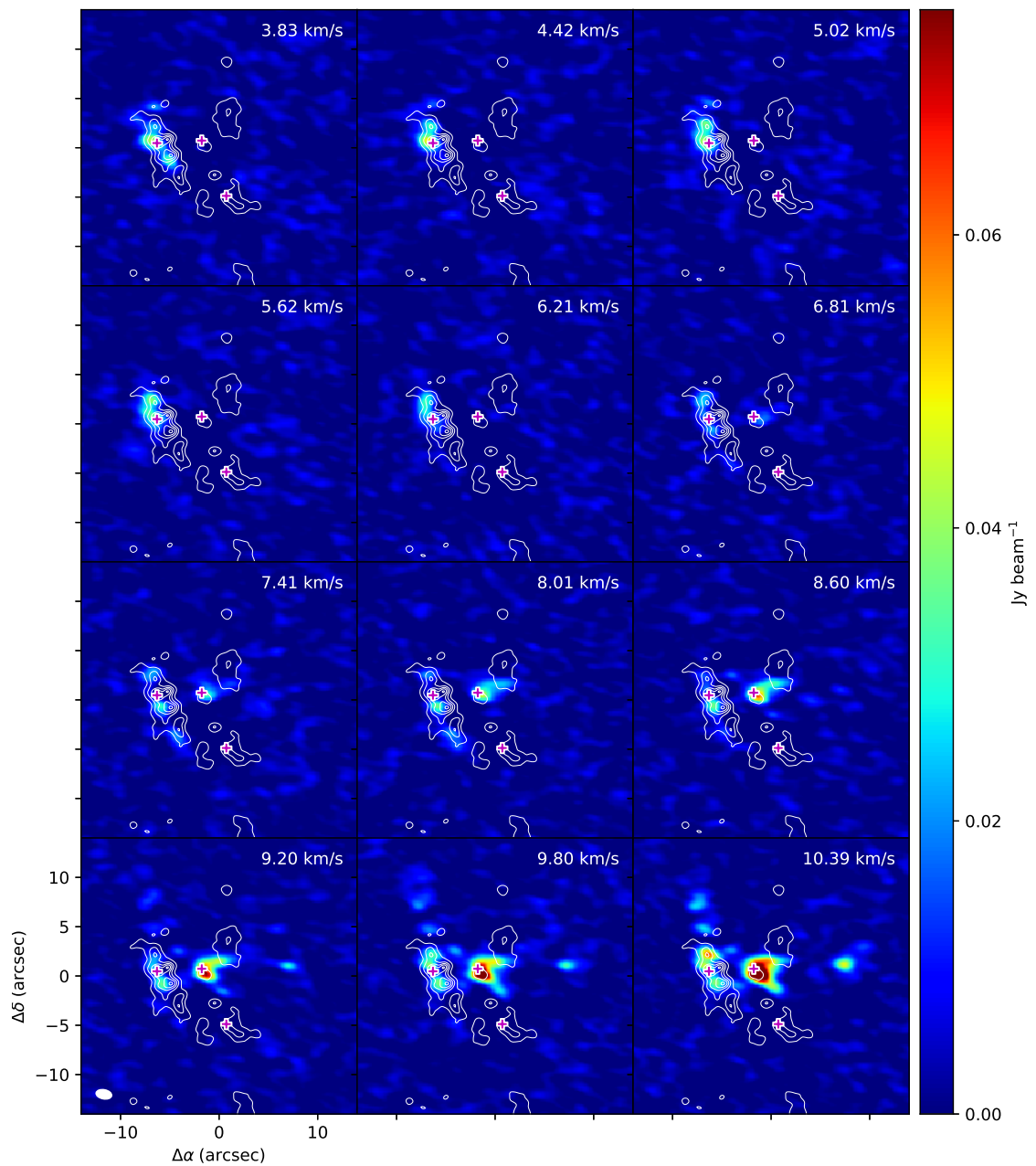


Figure 2.4: 245.202 GHz

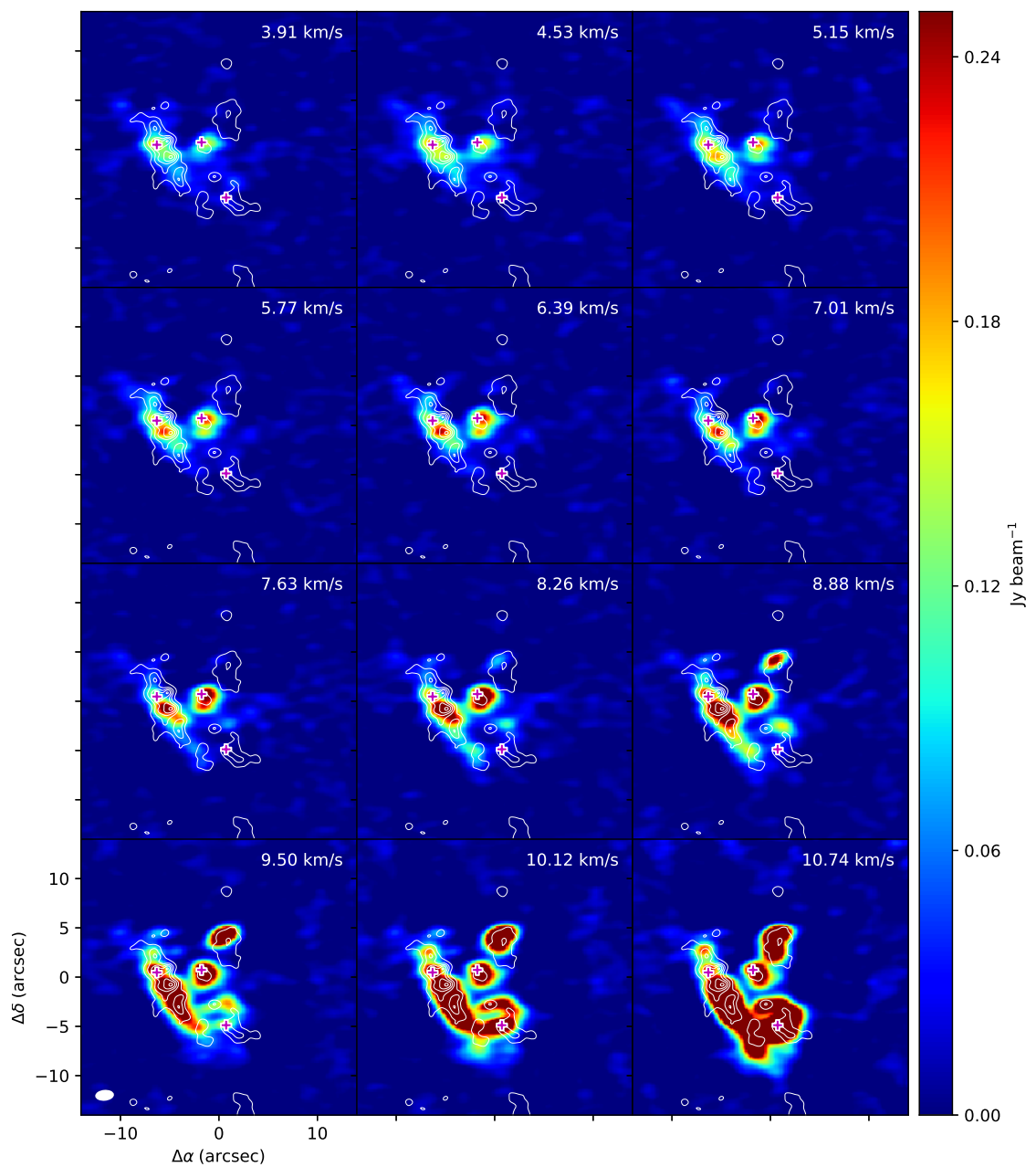


Figure 2.5: 235.735 GHz

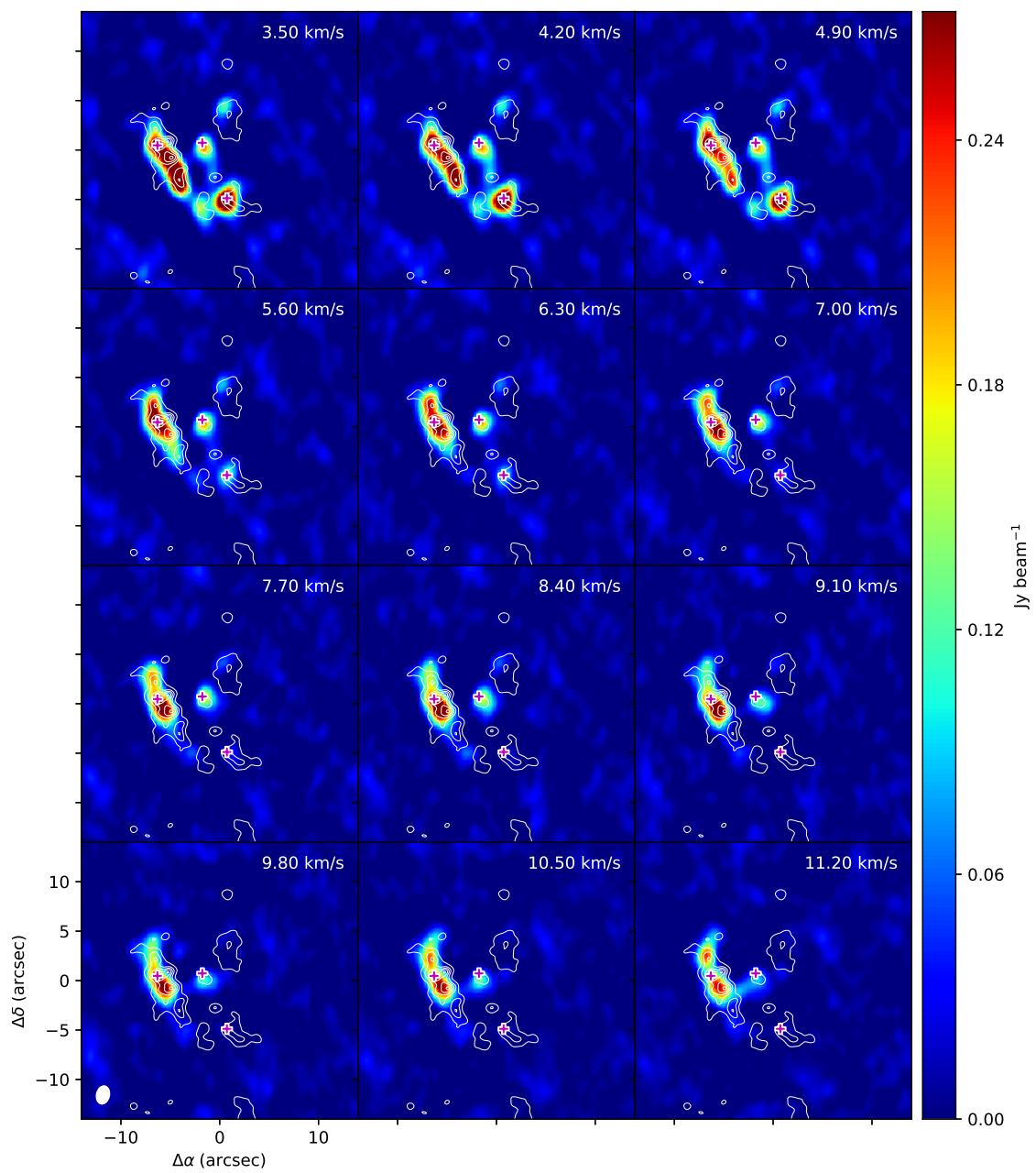


Figure 2.6: 242.262 GHz

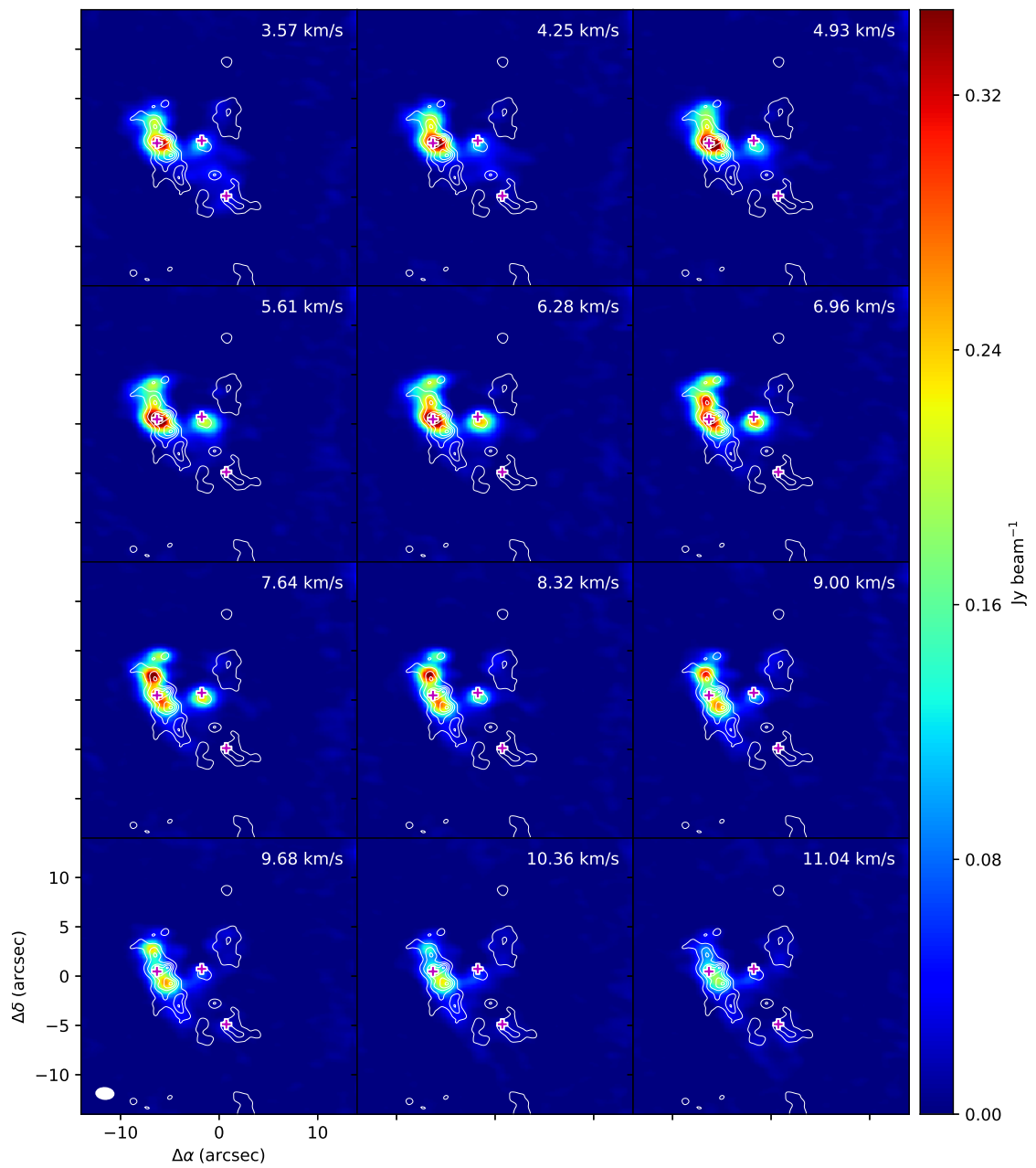


Figure 2.7: 215.670 GHz

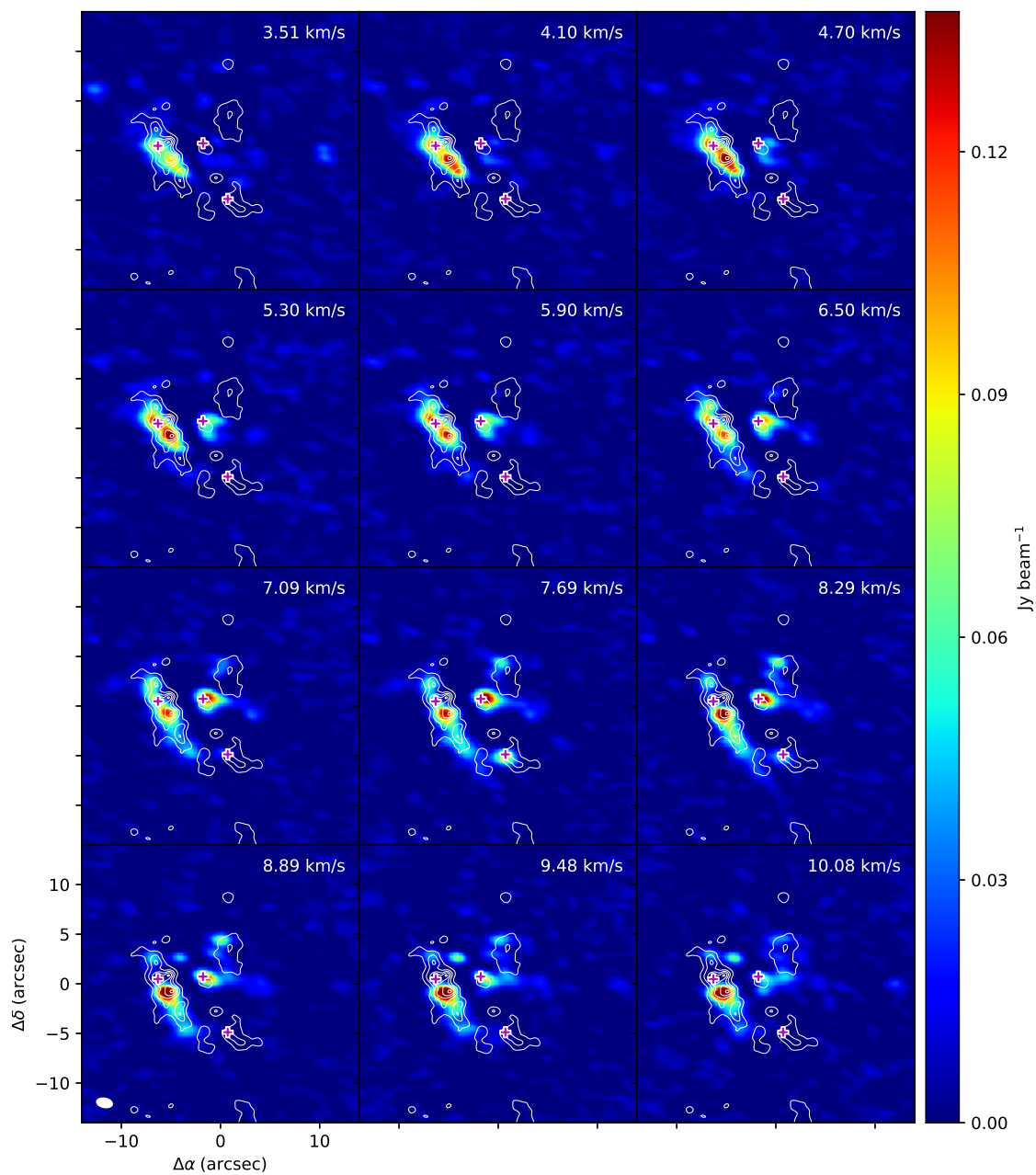


Figure 2.8: 244.887 GHz

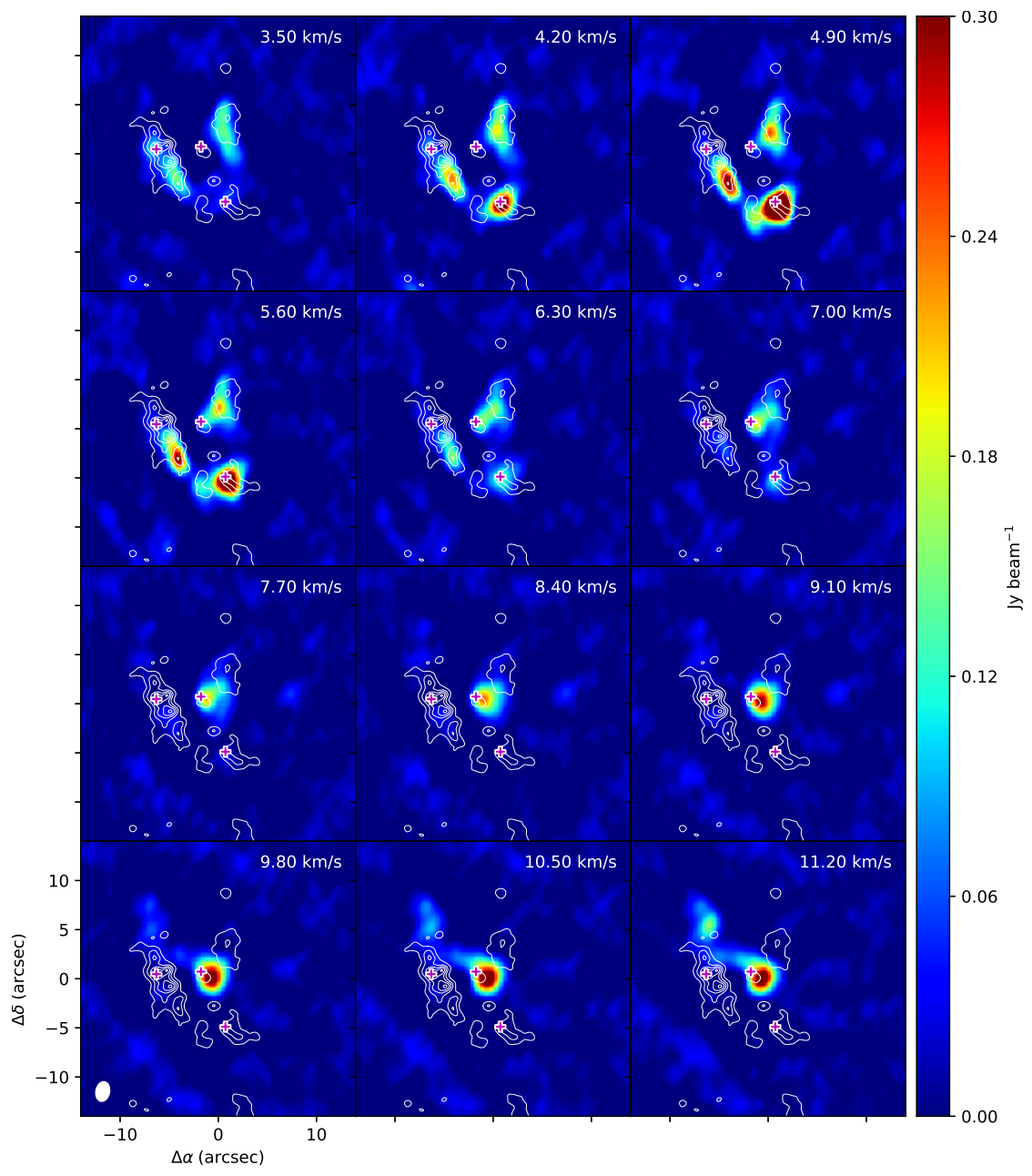


Figure 2.9: 221.755 GHz

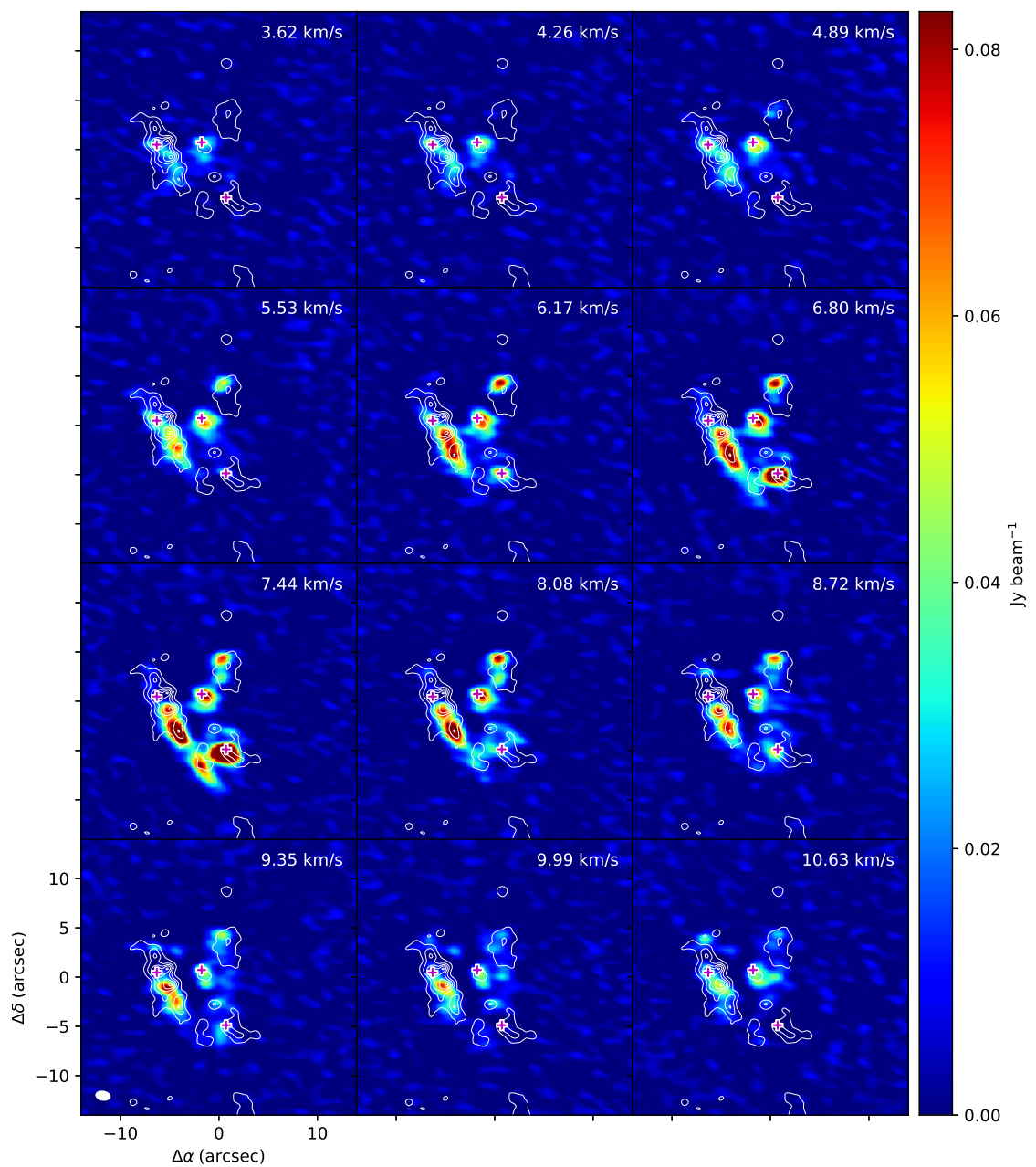


Figure 2.10: 229.908 GHz

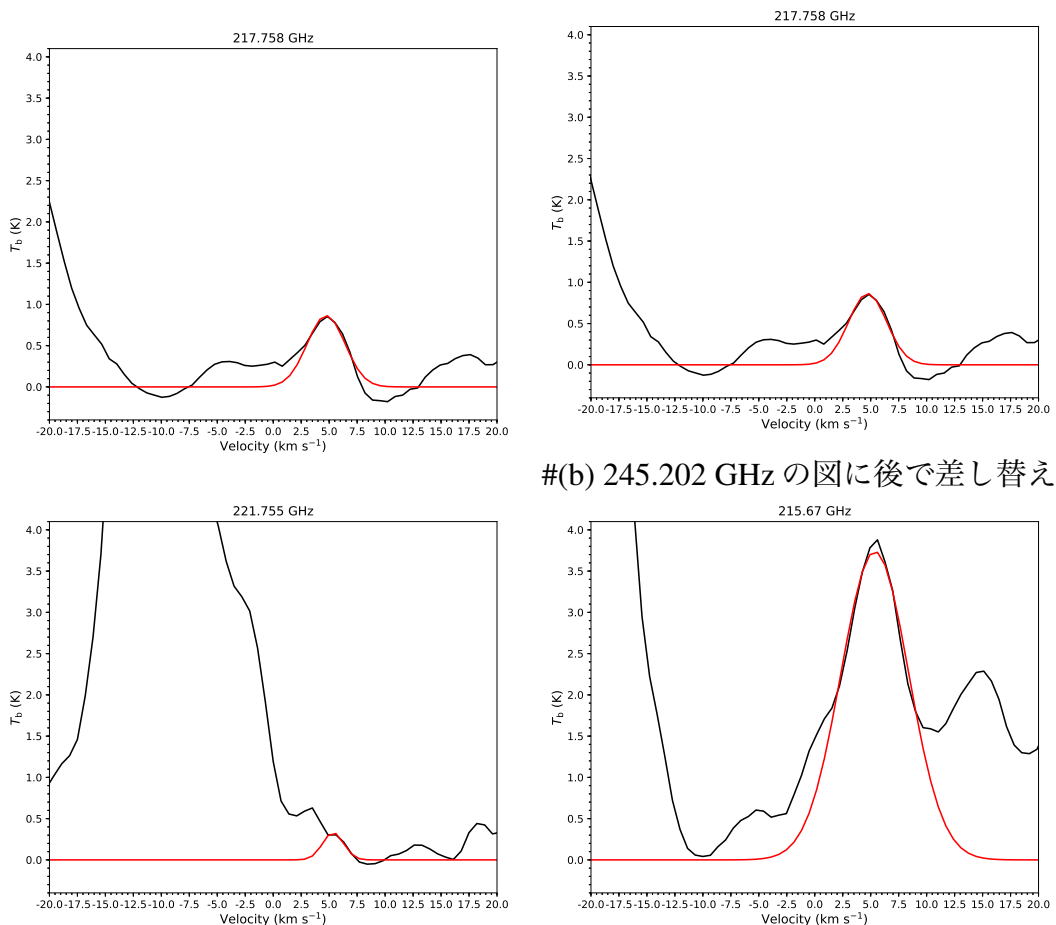


Figure 2.11: Spectrum

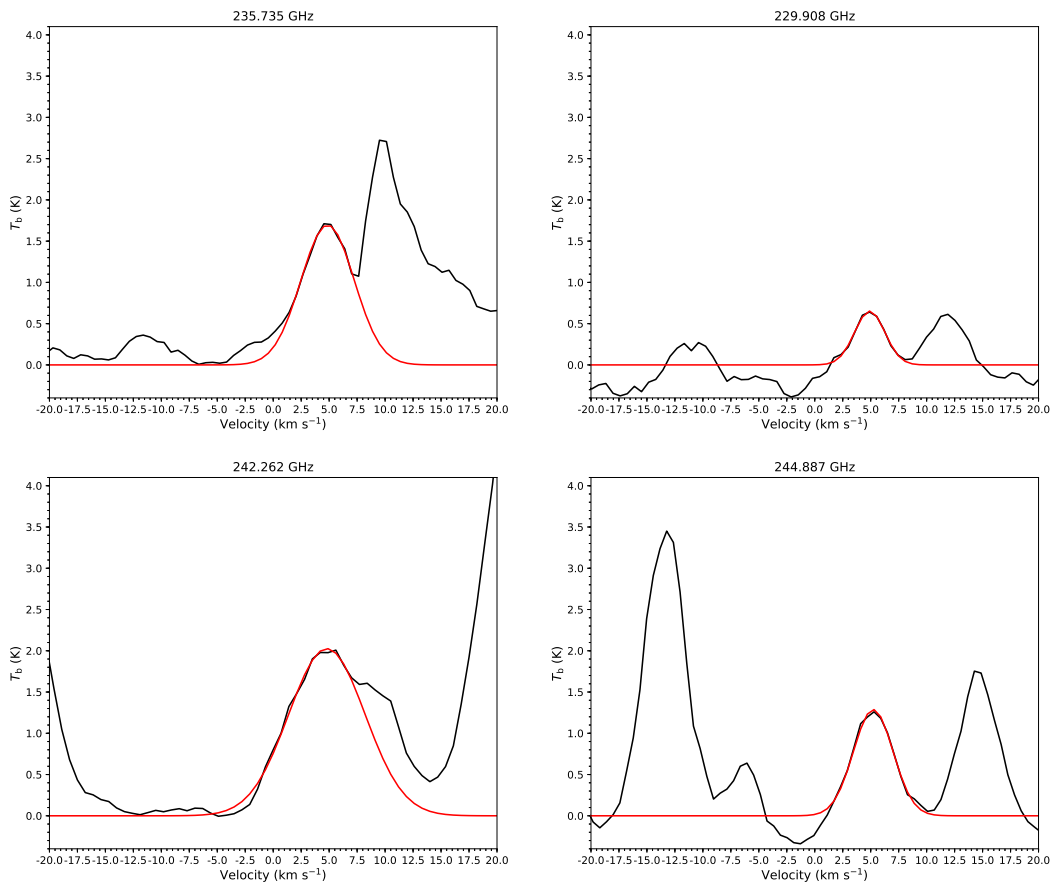


Figure 2.12: (Continued)

Chapter 3

Methylamine survey in low mass star-forming regions

3.1 Review of low mass star-forming region

3.2 Analysis

3.3 IRAS 16293

3.3.1 Observation data

3.3.2 Results

3.4 L483

3.4.1 Observation data

3.4.2 Results

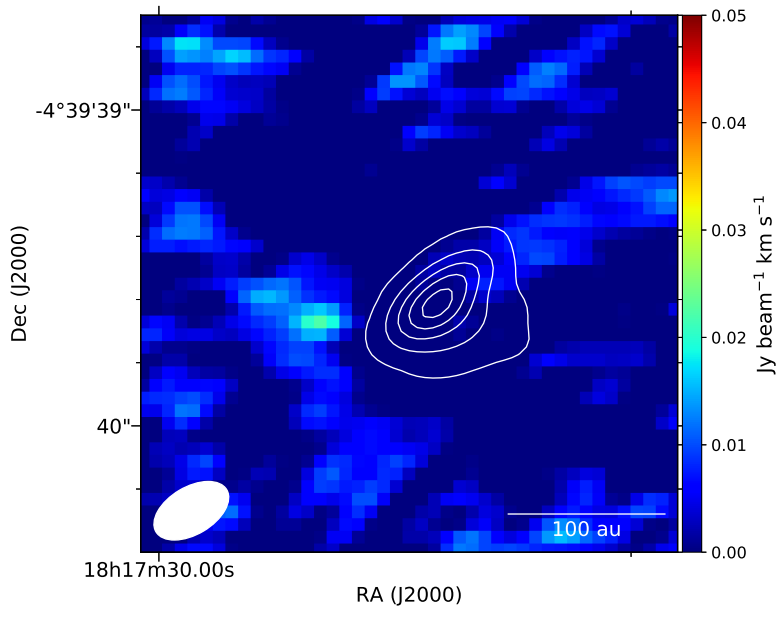


Figure 3.1: Integrated intensity map around 217.079 GHz. The white contours represent the 1.3 mm continuum map, where the contour levels are 10 %, 30 %, 50 %, 70 %, 90 % of the peak intensity.

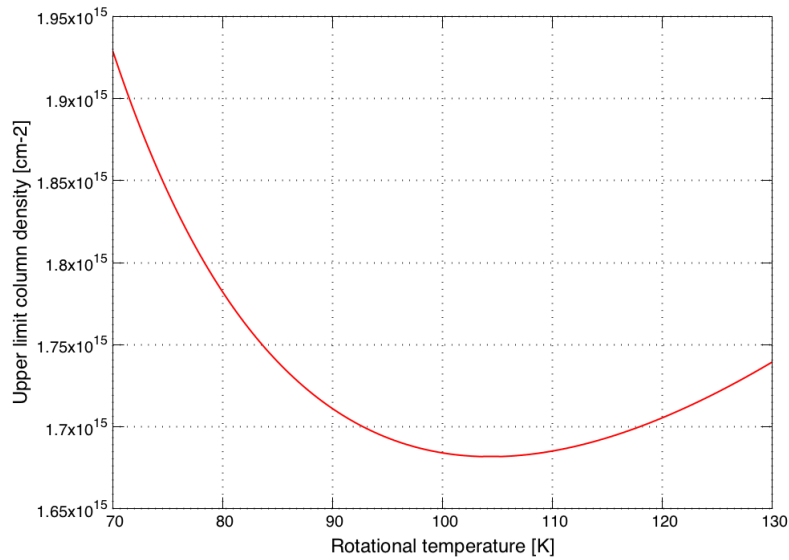


Figure 3.2: Upper limit column density for the strongest CH_3NH_2 transition ($11_2A_1 \rightarrow 11_2A_2$) as function of T_{rot} . A 3σ value of 75 Jy km s^{-1} is used.

Chapter 4

Discussion

Chapter 5

Conclusions

Appendix A

Distribution of methylamine lines contaminated by other molecular line emission in Orion-KL

A.1 Integrated intensity maps

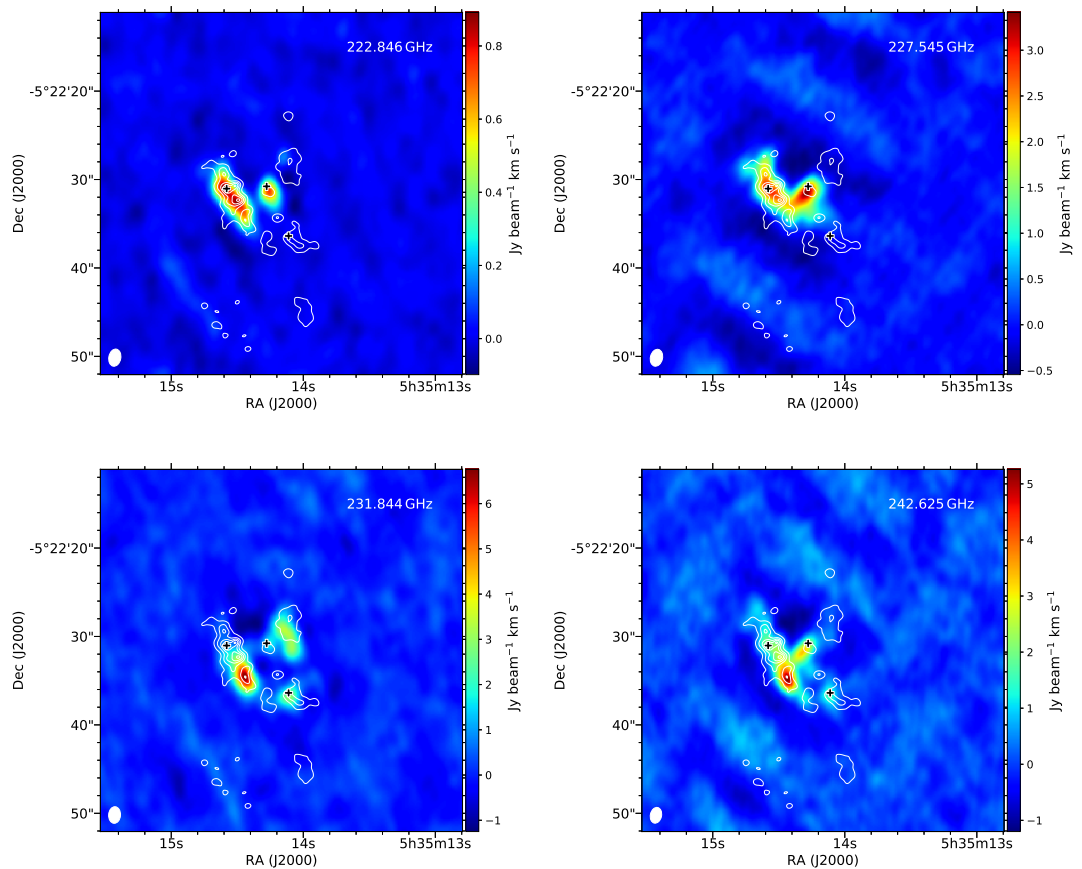


Figure A.1: Integrated intensity maps around methylamine line.

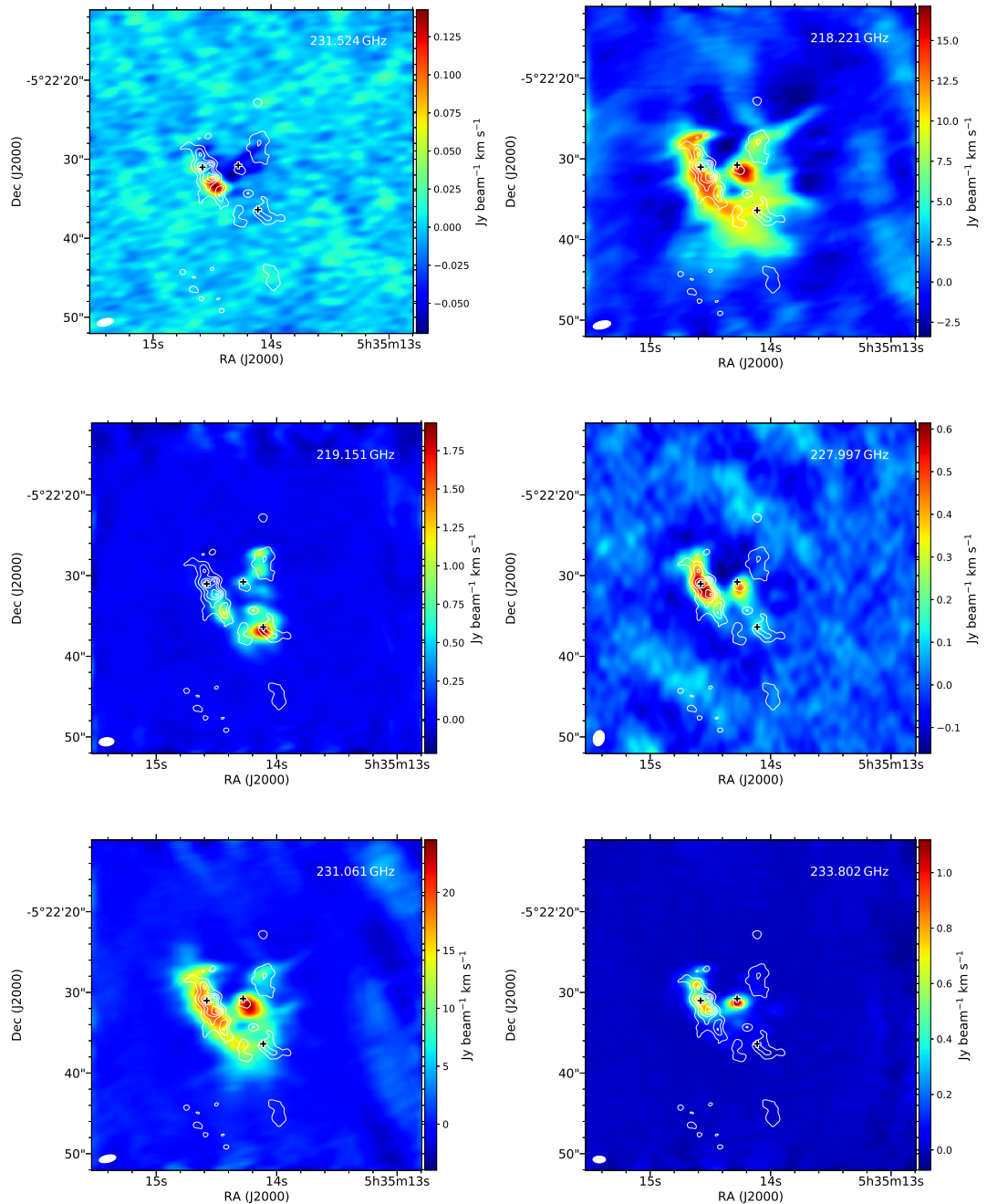


Figure A.2: (Continued)

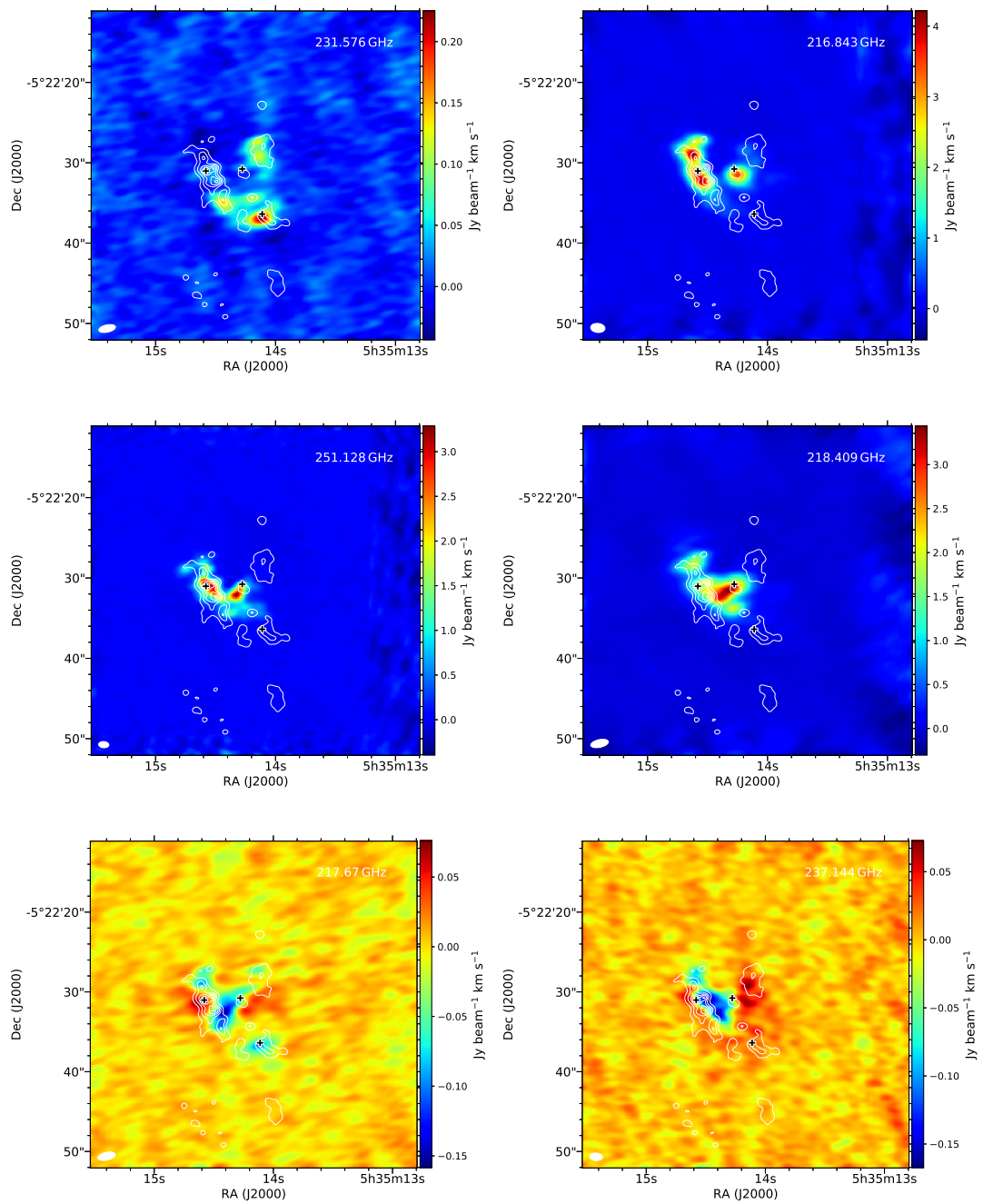


Figure A.3: (Continued)

A.2 Channel maps

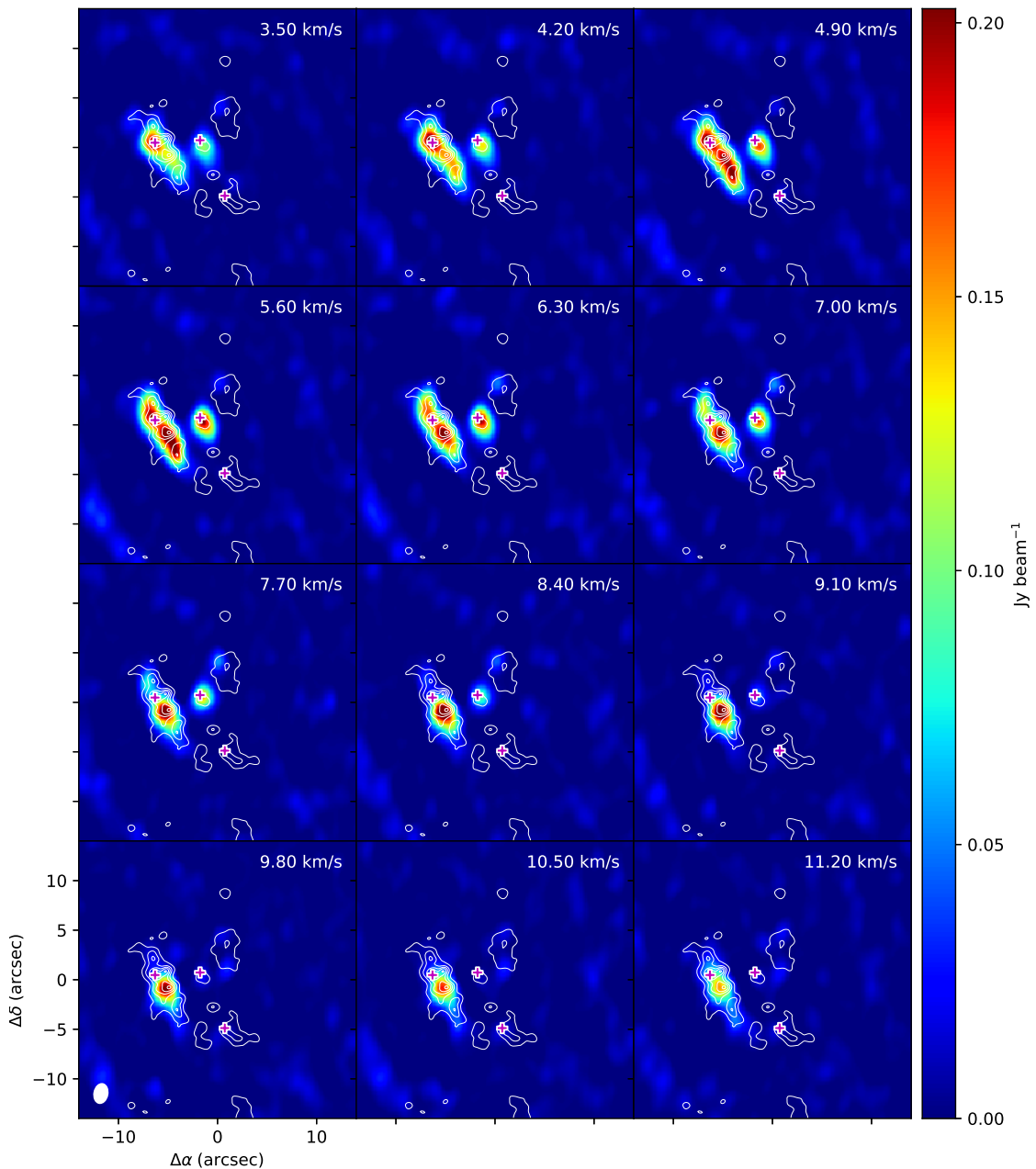


Figure A.4: 222.846GHz

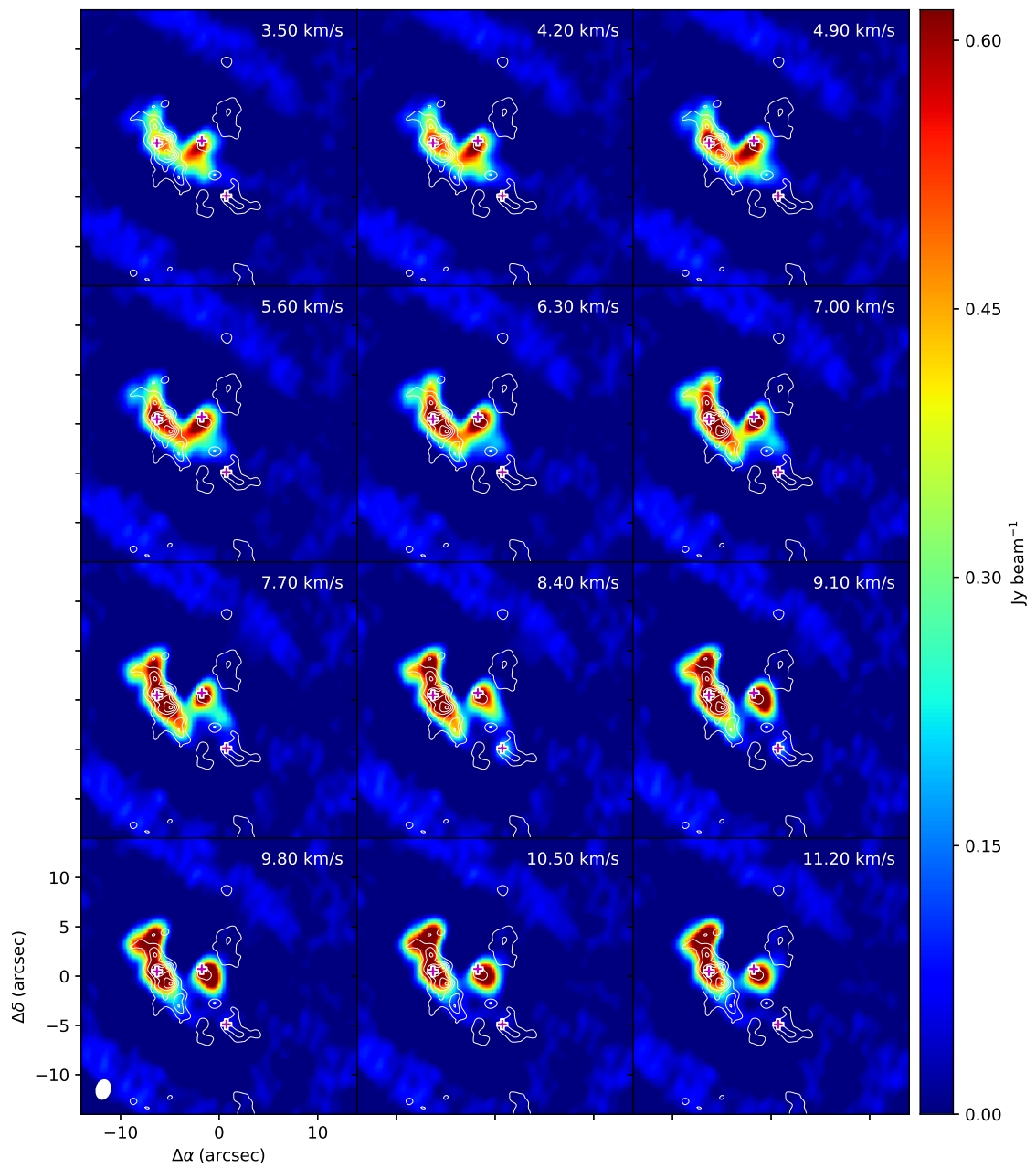


Figure A.5: 227.545GHz

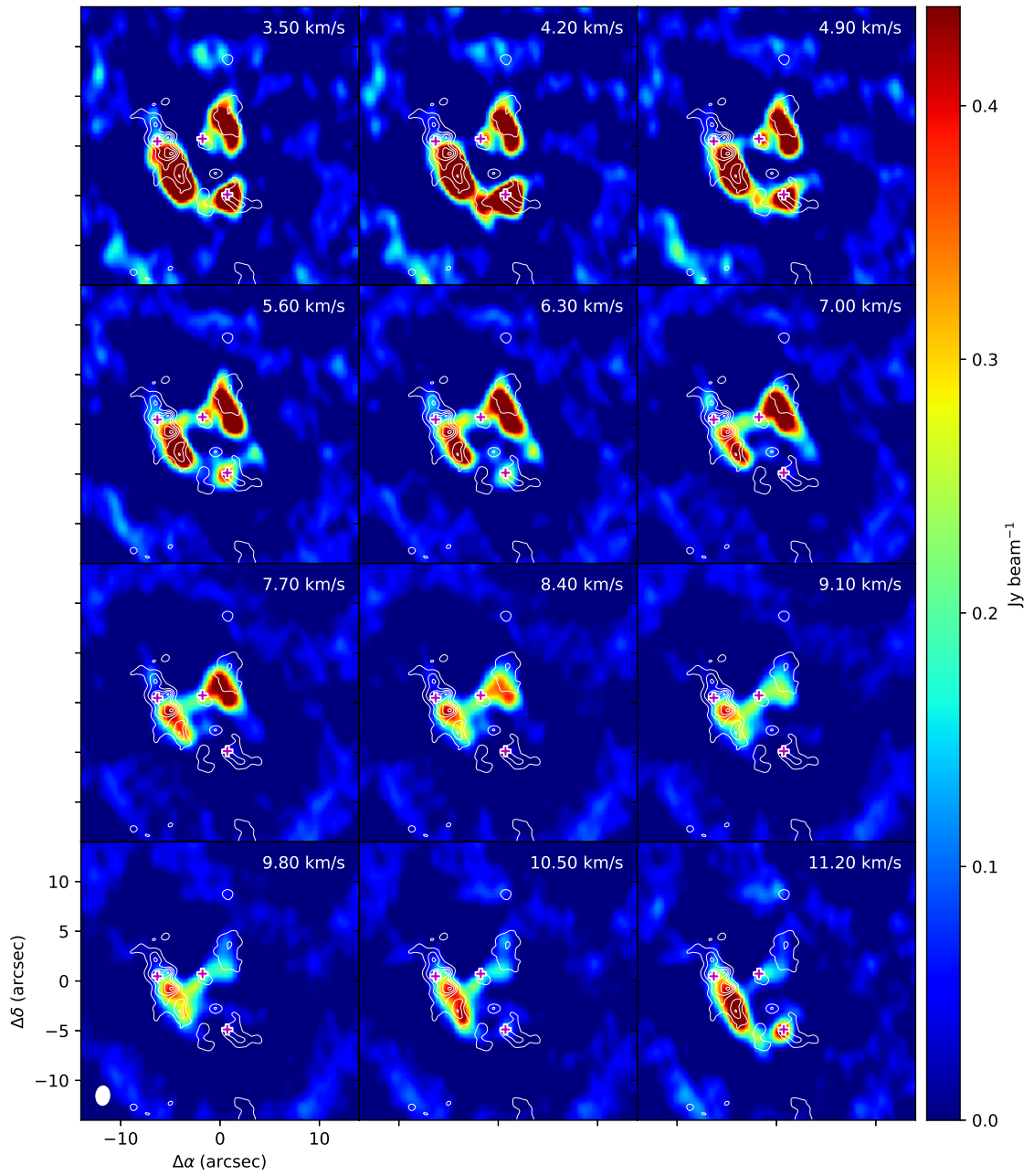


Figure A.6: 231.844GHz

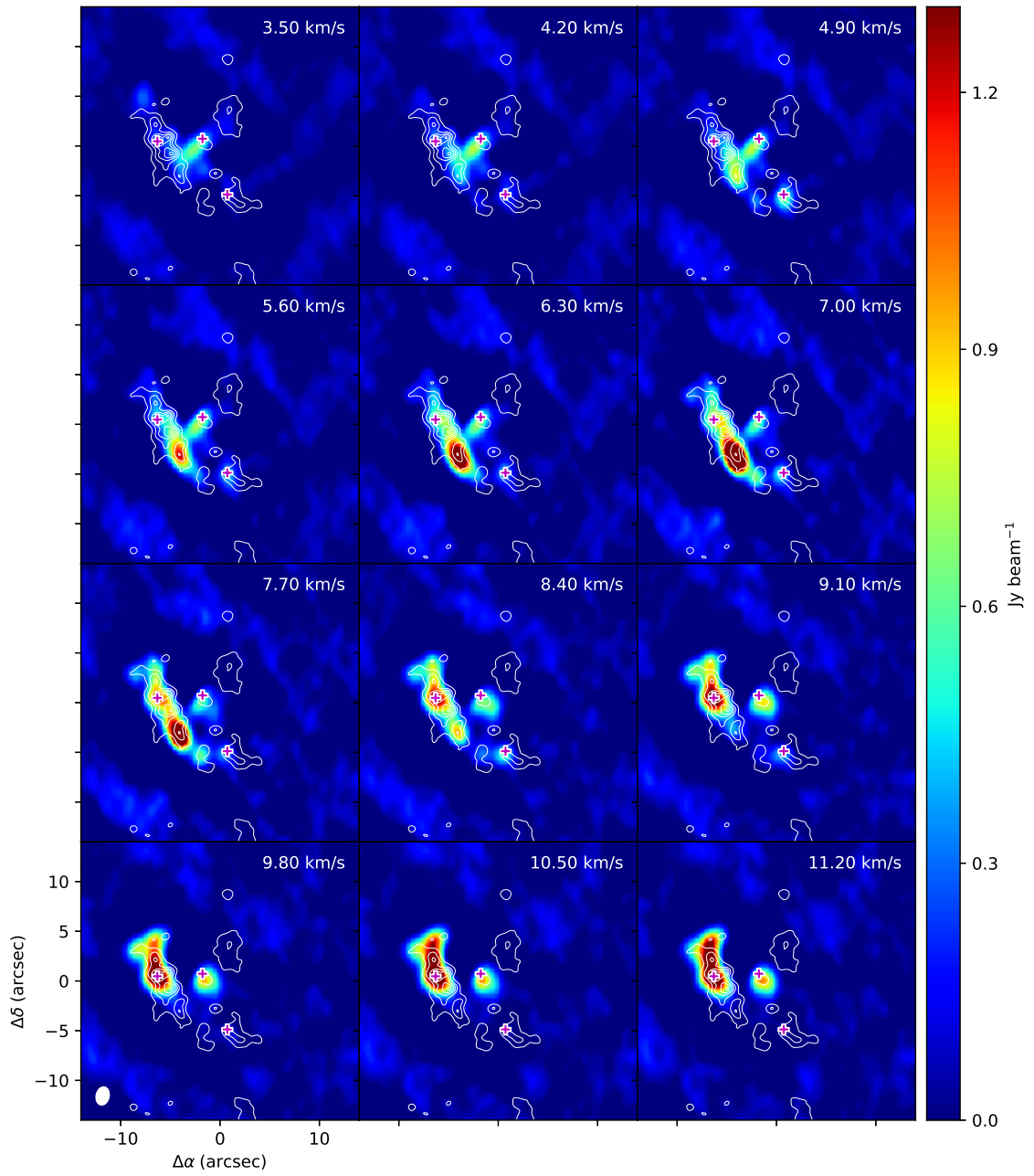


Figure A.7: 242.625GHz

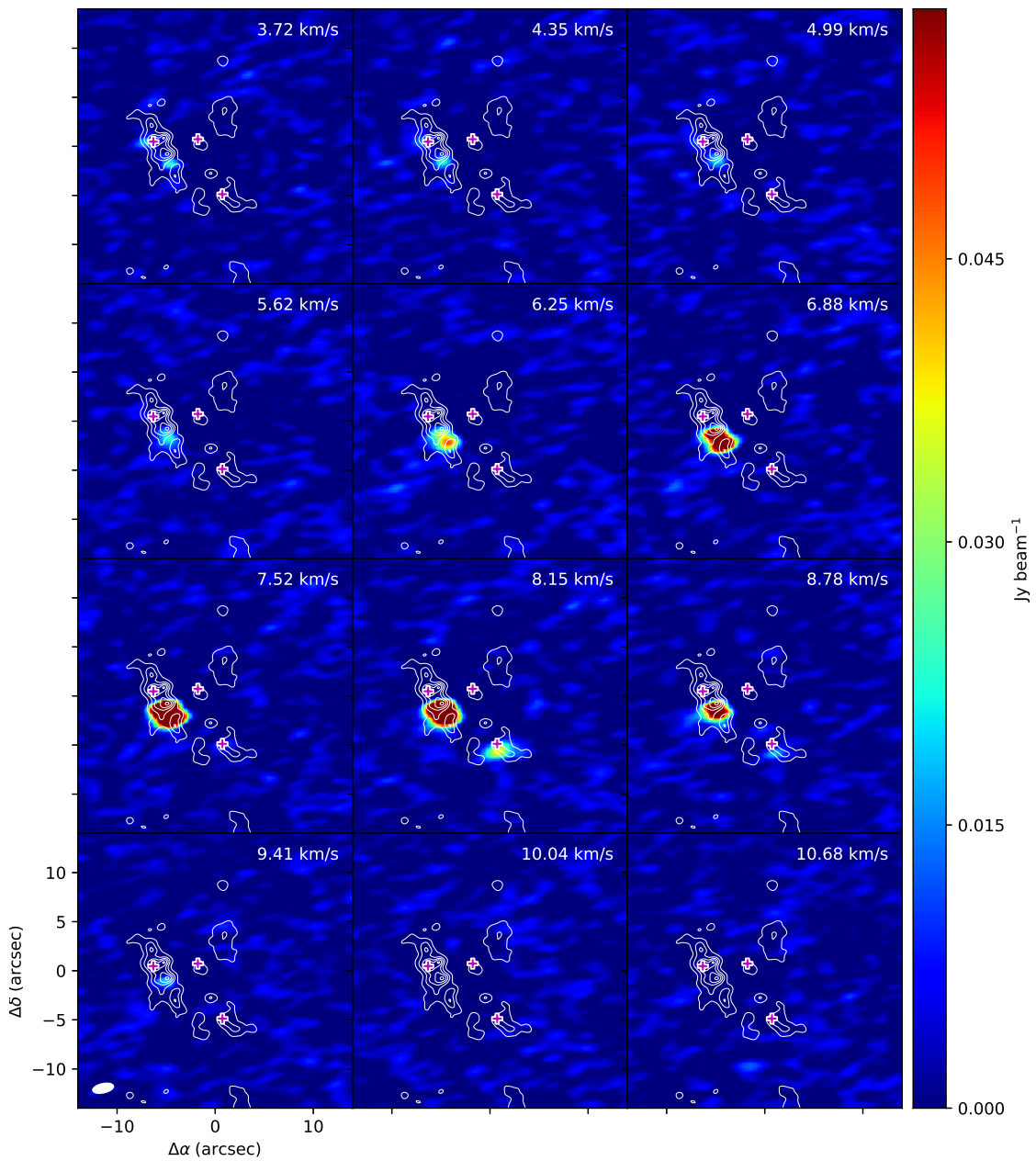


Figure A.8: 231.524GHz

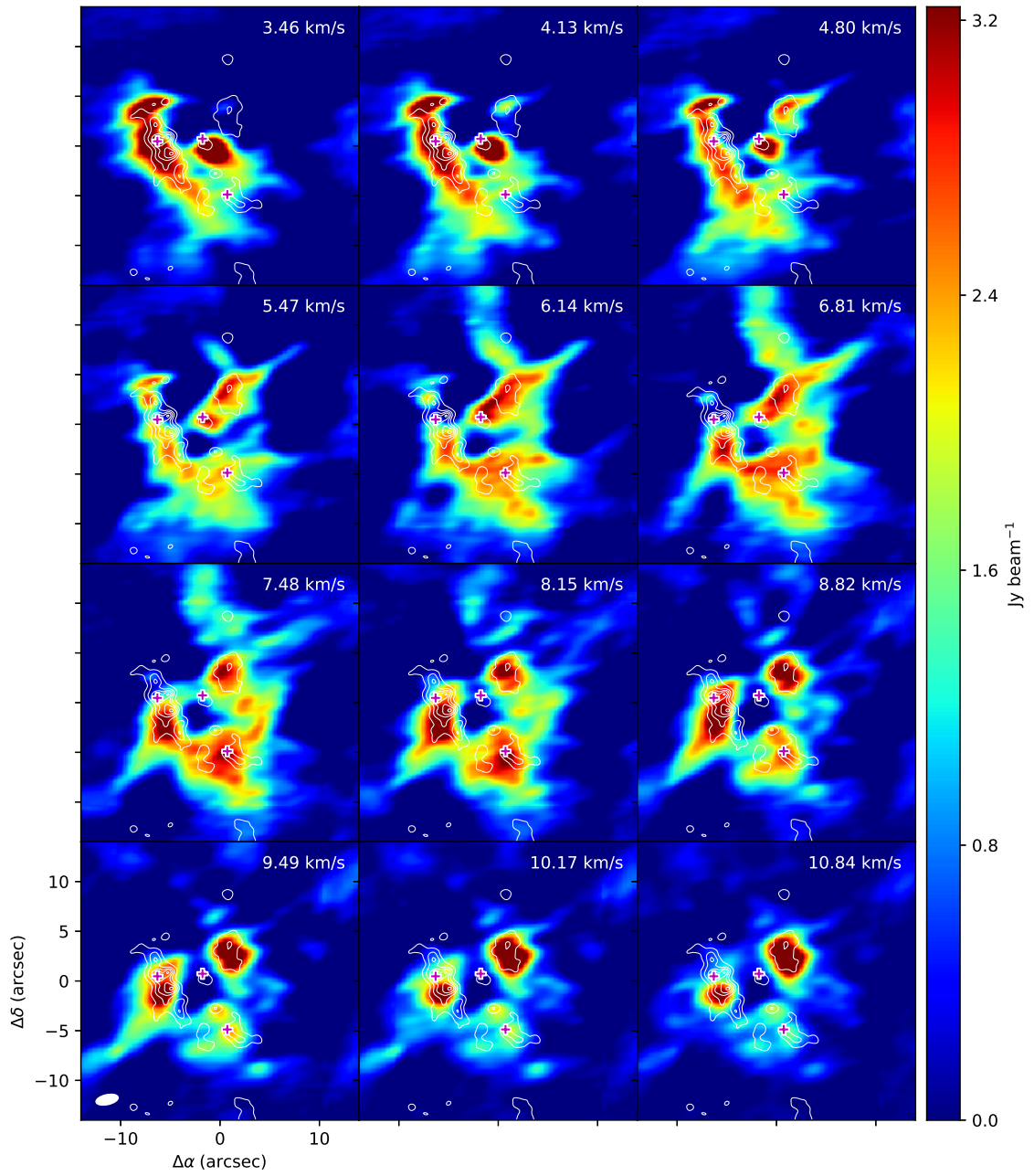


Figure A.9: 218.221GHz

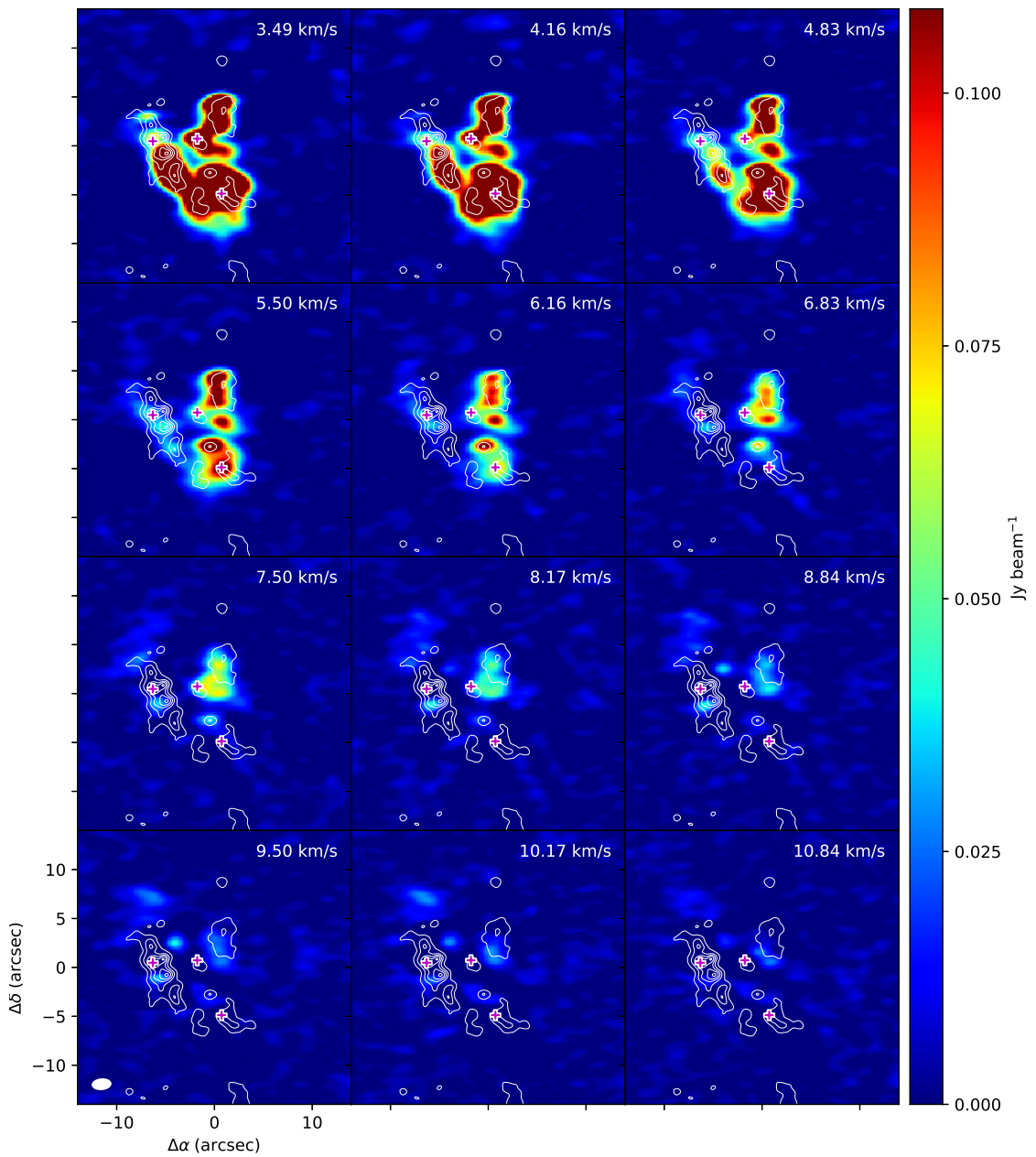


Figure A.10: 219.151GHz

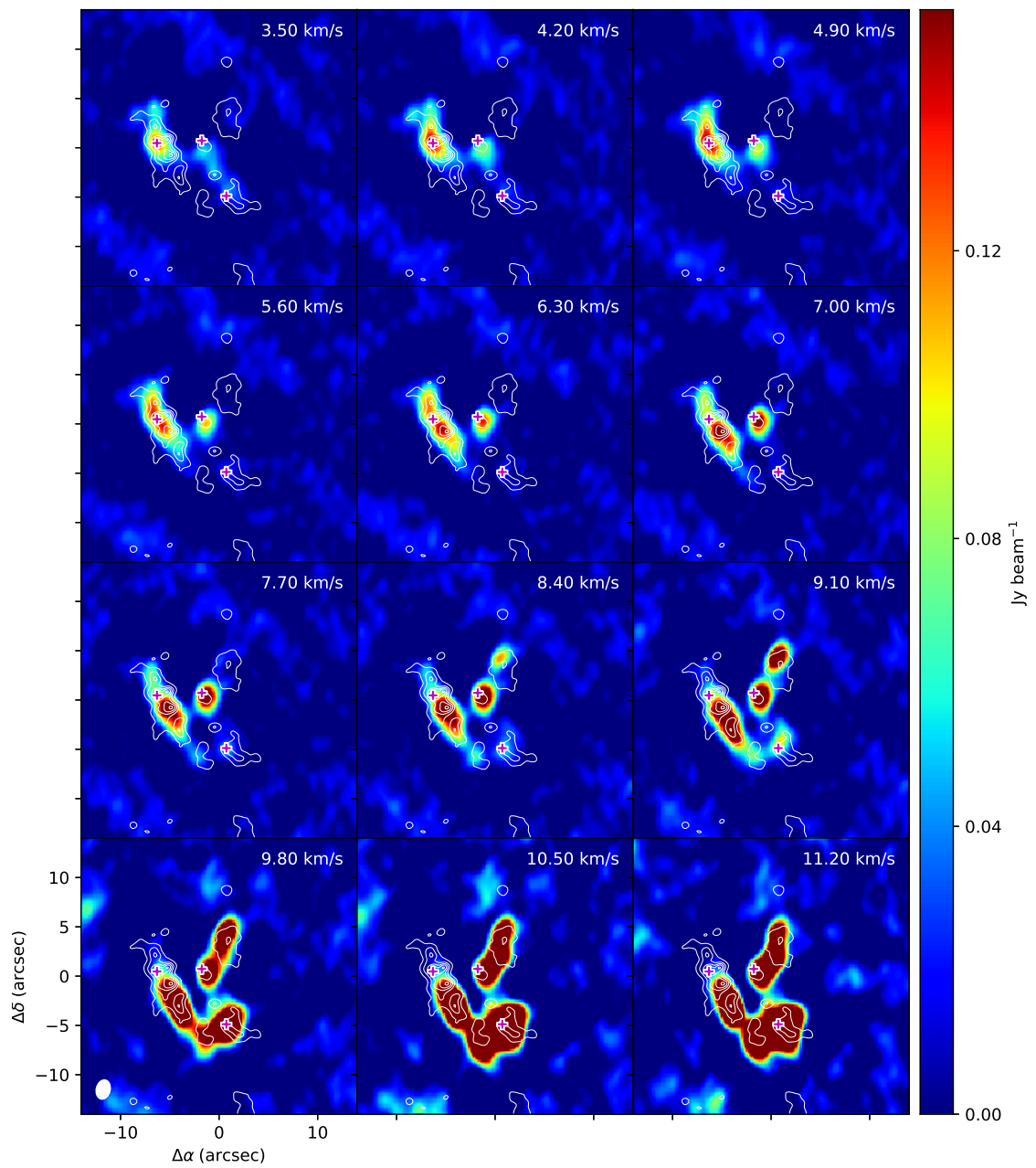


Figure A.11: 227.997GHz

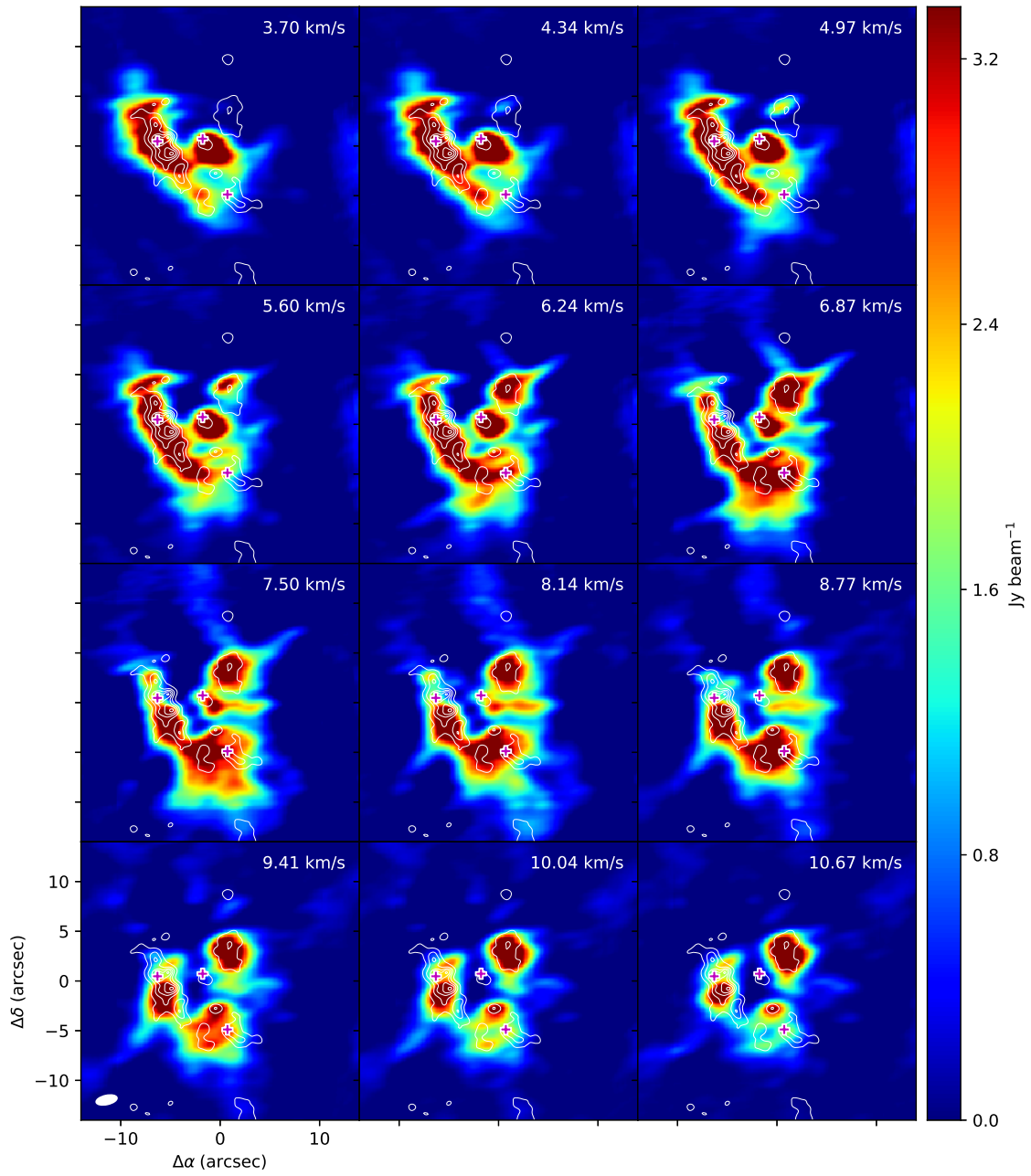


Figure A.12: 231.061GHz

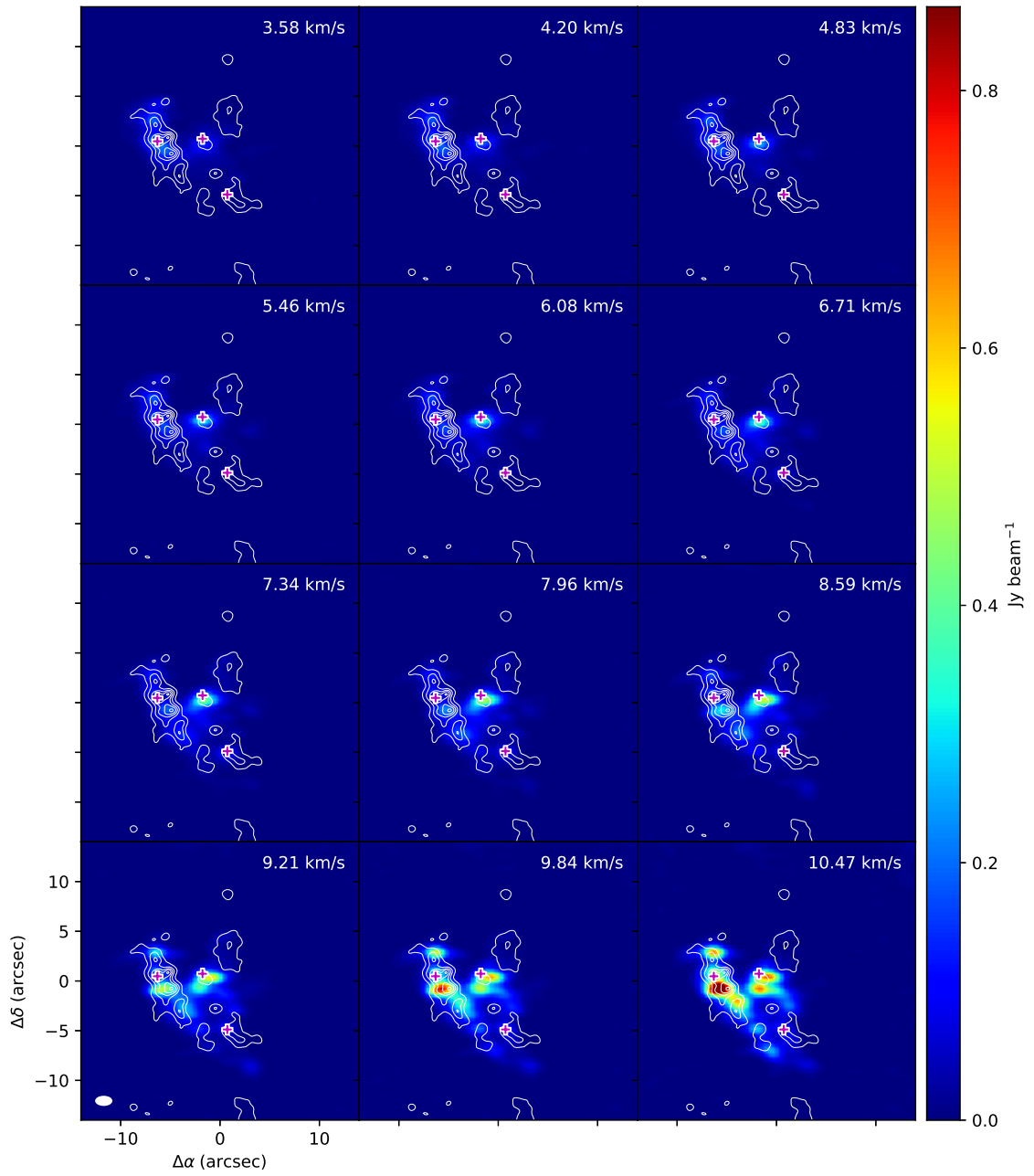


Figure A.13: 233.802GHz

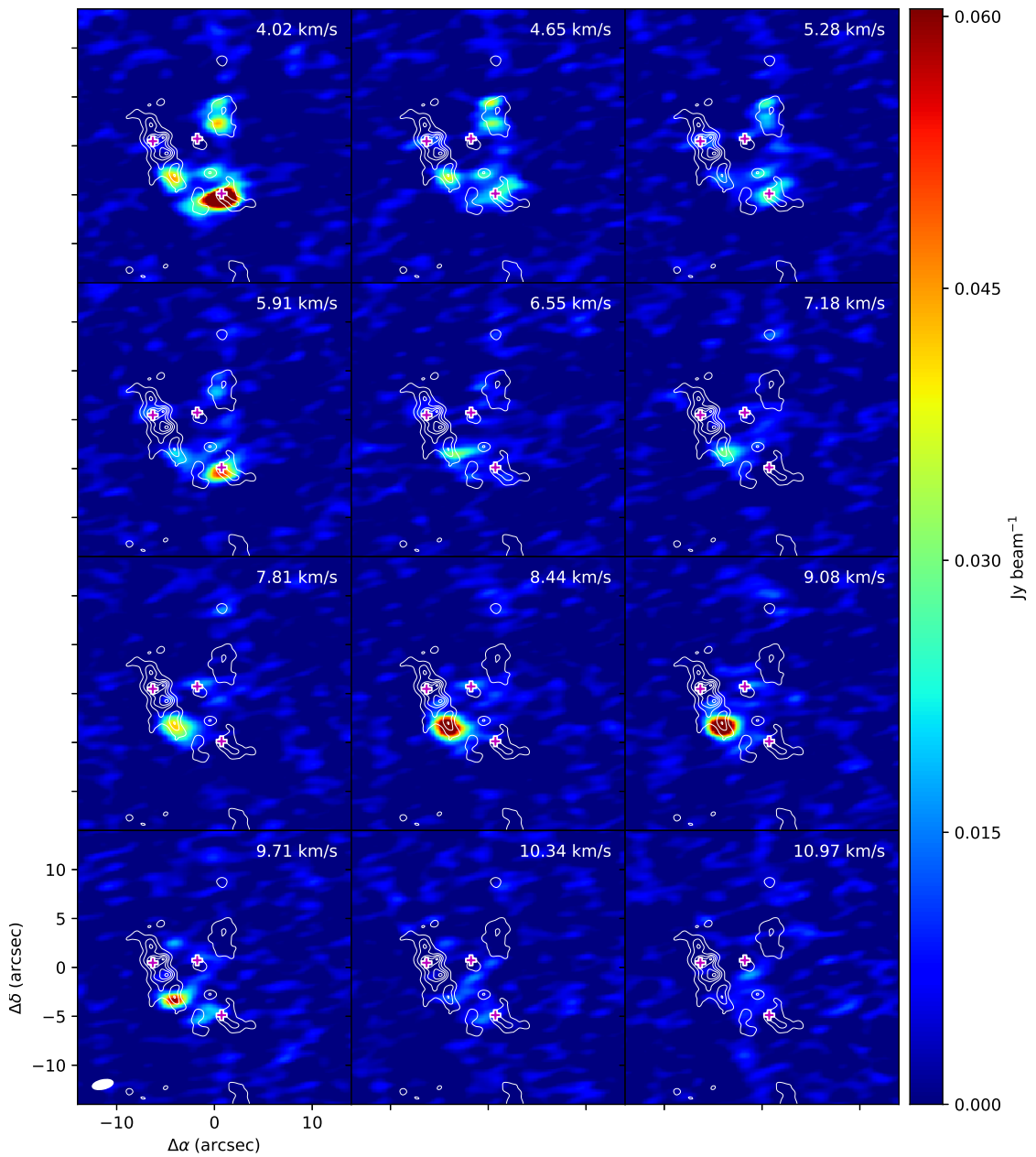


Figure A.14: 231.576GHz

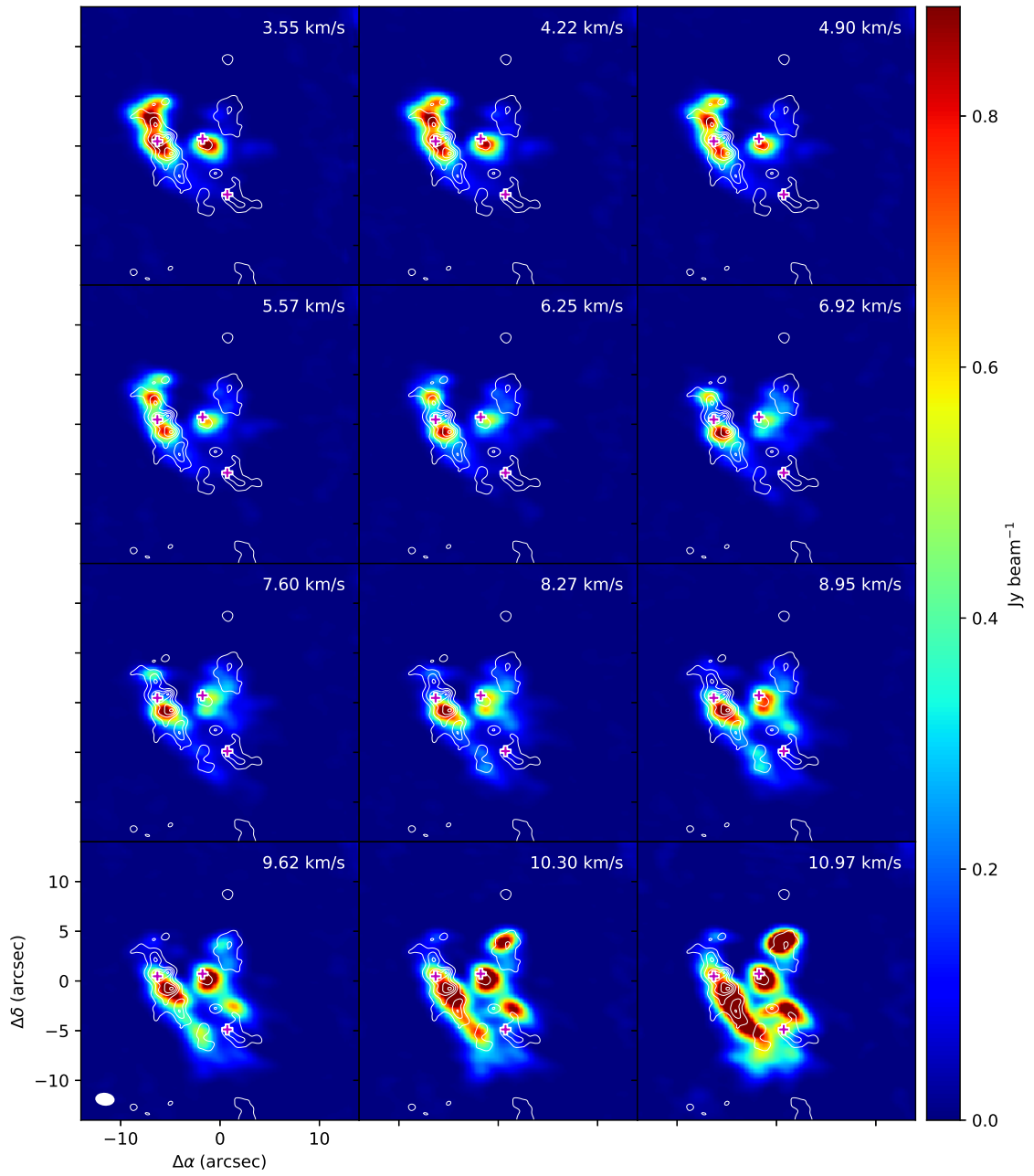


Figure A.15: 216.843GHz

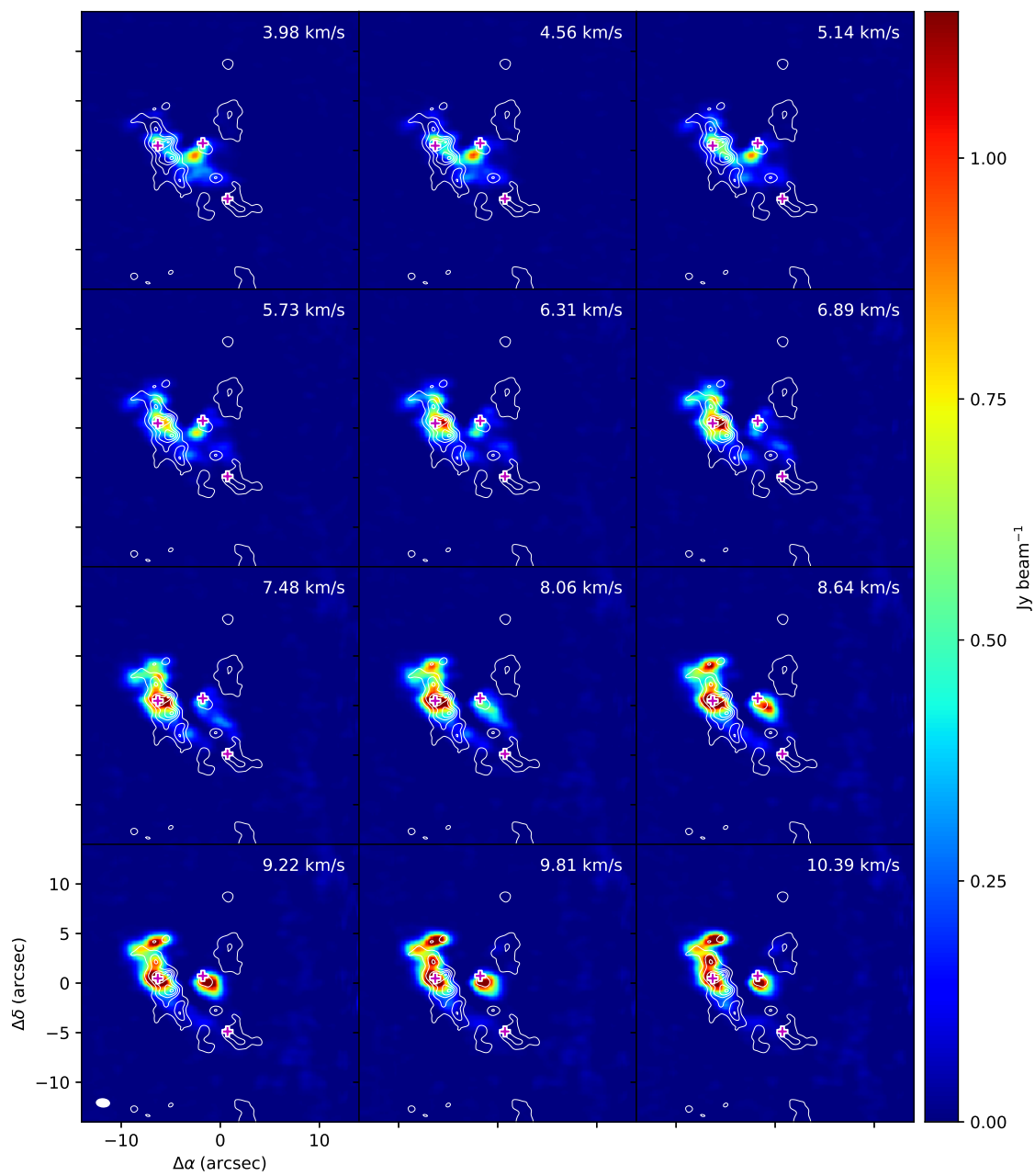


Figure A.16: 251.128GHz

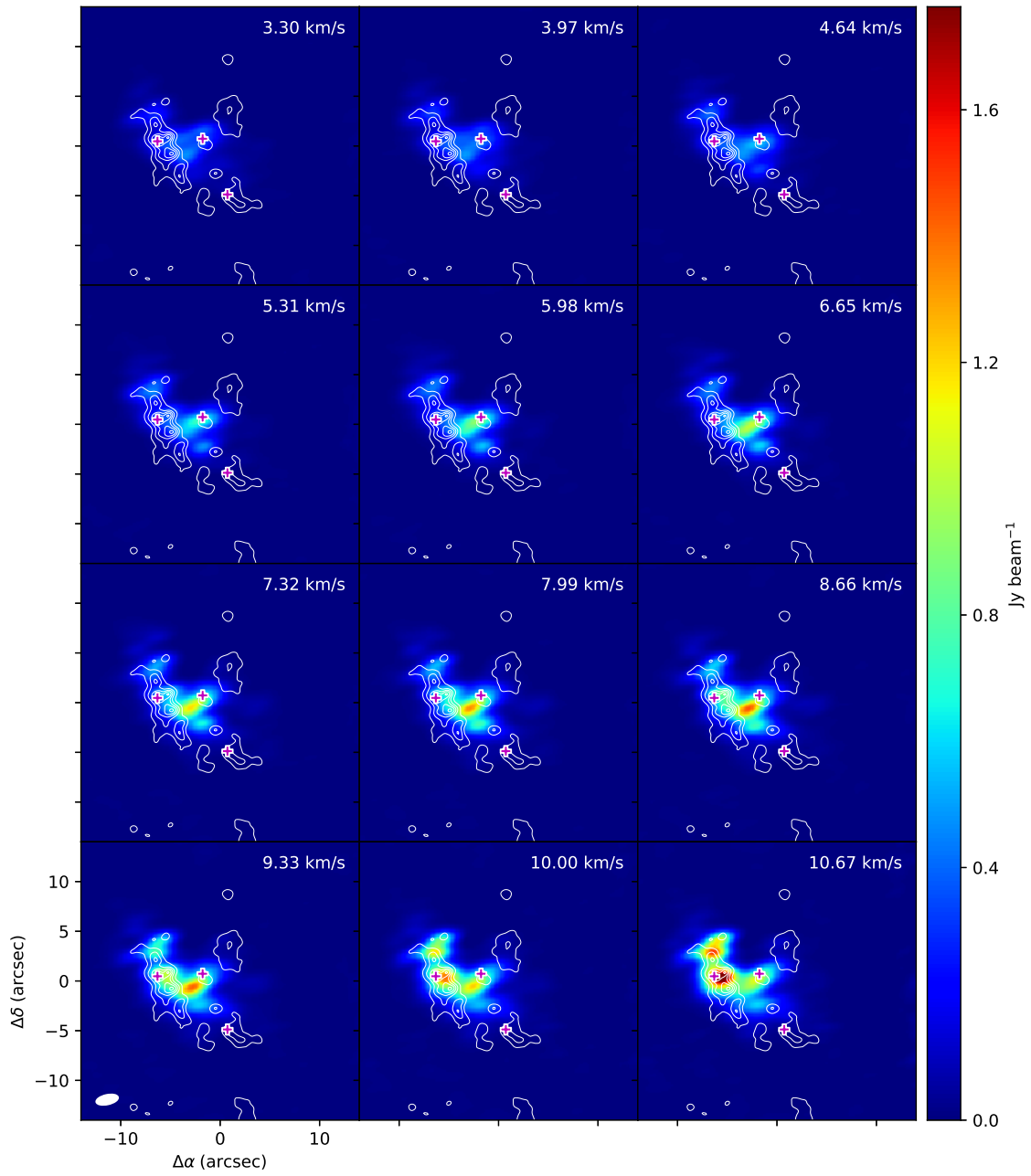


Figure A.17: 218.409GHz

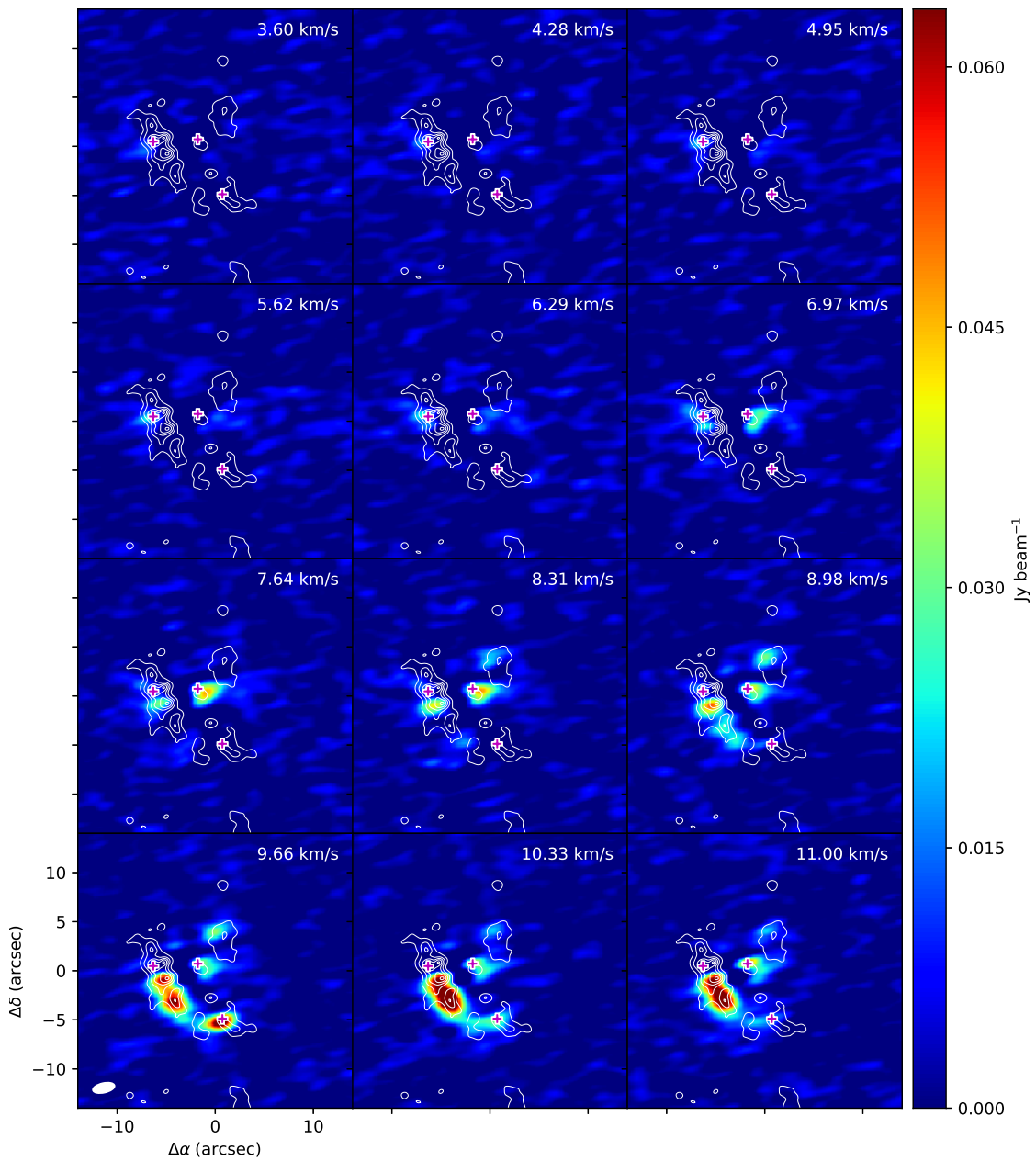


Figure A.18: 217.670GHz

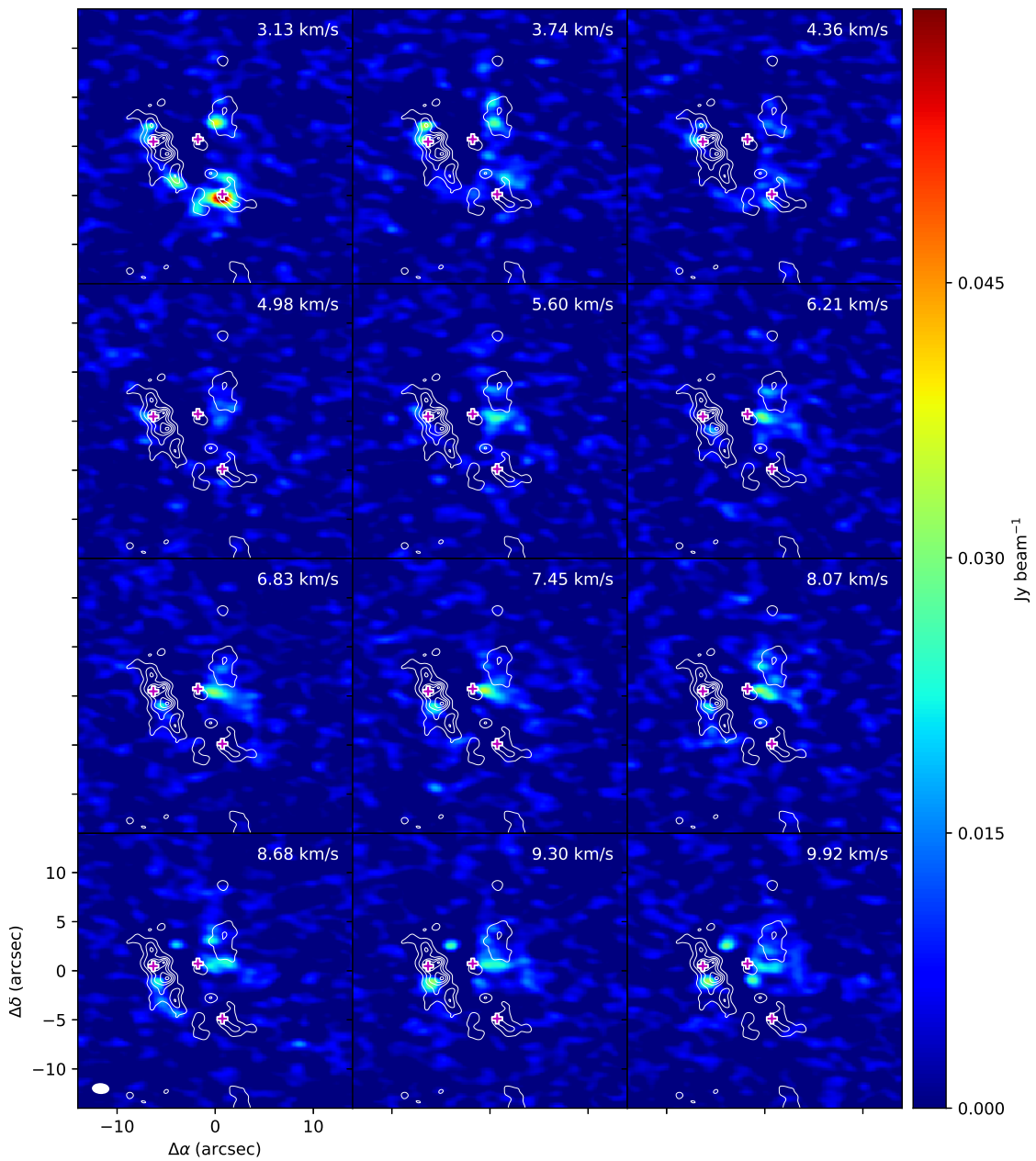


Figure A.19: 237.144GHz

Acknowledgments

References